This Accepted Manuscript has not been copyedited and formatted. The final version may differ from this version.

JNeurosci
THE JOURNAL OF NEUROSCIENCE

JNeurosci Accepted Manuscript

Research Articles: Systems/Circuits

ERK/MAPK signaling is required for pathway-specific striatal motor functions

Scott R. Hutton[1], James M. Otis[1], Erin M. Kim[1], Yashna Lamsal[1], Garret D. Stuber[1,2,3] and William D. Snider[1]

[1]*UNC Neuroscience Center*
[2]*Department of Psychiatry*
[3]*Department of Cell Biology and Physiology, University of North Carolina at Chapel Hill, Chapel Hill, NC, 27599, USA.*

DOI: 10.1523/JNEUROSCI.0473-17.2017

Received: 20 February 2017

Revised: 29 May 2017

Accepted: 1 July 2017

Published: 21 July 2017

Author contributions: S.R.H., J.M.O., G.S., and W.S. designed research; S.R.H., J.M.O., E.M.K., and Y.L. performed research; S.R.H., J.M.O., E.M.K., and Y.L. analyzed data; S.R.H., J.M.O., G.S., and W.S. wrote the paper.

Conflict of Interest: The authors declare no competing financial interests.

This work was supported by NIH Grants R01-NS031768 (WDS), R01-DA032750 (GDS), and F32-DA041184 (JMO). We thank the UNC Confocal and Multiphoton Imaging Core supported by NINDS Center Grant P30 NS045892, UNC Functional Genomics Core, and Viral Vector Core. We also thank Yaohong Wu for technical assistance.

Corresponding Author: William D. Snider, 115 Mason Farm Rd., NRB Rm 8109D CB #7250, Chapel Hill, NC 27599, william_snider@med.unc.edu

Cite as: J. Neurosci ; 10.1523/JNEUROSCI.0473-17.2017

Alerts: Sign up at www.jneurosci.org/cgi/alerts to receive customized email alerts when the fully formatted version of this article is published.

Accepted manuscripts are peer-reviewed but have not been through the copyediting, formatting, or proofreading process.

Copyright © 2017 the authors

JNeurosci Accepted Manuscript

1 **ERK/MAPK signaling is required for pathway-specific striatal motor functions**

2

3 Abbreviated Title: Conditional ERK deletion in medium spiny neurons

4

5 Scott R. Hutton[1], James M. Otis[1], Erin M. Kim[1], Yashna Lamsal[1], Garret D. Stuber[1,2,3], William
6 D. Snider[1]

7

8 [1]UNC Neuroscience Center; [2]Department of Psychiatry; [3]Department of Cell Biology and
9 Physiology, University of North Carolina at Chapel Hill, Chapel Hill, NC, 27599, USA.

10

11 Corresponding Author: William D. Snider, 115 Mason Farm Rd., NRB Rm 8109D CB #7250,
12 Chapel Hill, NC 27599, william_snider@med.unc.edu

13

14 Number of Pages: 46
15 Number of Figures: 7
16 Number of Tables: 1
17 Number of words (abstract): 188
18 Number of words (introduction): 629
19 Number of words (discussion): 1489
20 Conflict of Interest: The authors declare no competing financial interests.

21 Acknowledgements: This work was supported by NIH Grants R01-NS031768 (WDS), R01-
22 DA032750 (GDS), and F32-DA041184 (JMO). We thank the UNC Confocal and Multiphoton
23 Imaging Core supported by NINDS Center Grant P30 NS045892, UNC Functional Genomics
24 Core, and Viral Vector Core. We also thank Yaohong Wu for technical assistance.

JNeurosci Accepted Manuscript

Abstract

The ERK/MAPK intracellular signaling pathway is hypothesized to be a key regulator of striatal activity via modulation of synaptic plasticity and gene transcription. However, prior investigations into striatal ERK/MAPK functions have yielded conflicting results. Further, these studies have not delineated the cell type-specific roles of ERK/MAPK signaling due to the reliance on globally-administered pharmacological ERK/MAPK inhibitors and the use of genetic models that only partially reduce total ERK/MAPK activity. Here, we generated mouse models in which ERK/MAPK signaling was completely abolished in each of the two distinct classes of medium spiny neurons (MSNs). ERK/MAPK deletion in D1R-MSNs (direct pathway) resulted in decreased locomotor behavior, reduced weight gain, and early postnatal lethality. In contrast, loss of ERK/MAPK signaling in D2R-MSNs (indirect-pathway) resulted in a profound hyperlocomotor phenotype. ERK/MAPK-deficient D2R-MSNs exhibited a significant reduction in dendritic spine density, markedly suppressed electrical excitability, and suppression of activity associated gene expression– even after pharmacological stimulation. Our results demonstrate the importance of ERK/MAPK signaling in governing the motor functions of the striatal direct and indirect pathways. Our data further show a critical role for ERK in maintaining the excitability and plasticity of D2R-MSNs.

JNeurosci Accepted Manuscript

43 **Significance Statement**

44 Alterations in ERK/MAPK activity are associated with drug abuse, as well as neuropsychiatric
45 and movement disorders. However, genetic evidence defining the functions of ERK/MAPK
46 signaling in striatum-related neurophysiology and behavior is lacking. We show that loss of
47 ERK/MAPK signaling leads to pathway-specific alterations in motor function, reduced neuronal
48 excitability, and the inability of medium spiny neurons to regulate activity-induced gene
49 expression. Our results underscore the potential importance of the ERK/MAPK pathway in
50 human movement disorders.

51

JNeurosci Accepted Manuscript

52 **Introduction**

53 The basal ganglia govern a vast array of psychomotor behaviors (Nelson and Kreitzer,
54 2014; Graybiel and Grafton, 2015). Sensorimotor information is integrated into the basal ganglia
55 via the striatum, where glutamatergic and dopaminergic inputs converge onto two distinct
56 classes of medium spiny neurons (MSNs) (Gerfen et al., 1990; Kawaguchi et al., 1990; Gong et
57 al., 2007; Cerovic et al., 2013). Direct-pathway MSNs (D1R-MSNs) express the dopamine 1
58 receptor (D1) and largely project to the substantia nigra reticulata (SNr) and globus pallidus
59 internae (GPi). Indirect-pathway MSNs (D2R-MSNs) express dopamine 2 (D2) and adenosine
60 A2a (A2a) receptors, and predominantly target the globus pallidus externae (GPe).
61 Experimental evidence suggests that D1R- and D2R-MSN activities have opposing actions. In
62 the motor system, stimulation of the direct pathway elicits activation of motor behaviors whereas
63 stimulation of the indirect pathway inhibits motor activity (Kravitz et al., 2010; Farrell et al.,
64 2013). Silencing each pathway has converse effects (Durieux et al., 2009; Hikida et al., 2010).

65 The convergence of glutamatergic and dopaminergic signaling onto MSNs leads to long-
66 term alterations in neuronal excitability, changes in activity-induced gene expression, and
67 modulation of dendritic spine density (Cerovic et al., 2013; Nelson and Kreitzer, 2014). A major
68 signaling pathway implicated in mediating these long-lasting changes is ERK/MAPK (ERK)
69 (Thomas and Huganir, 2004; Pascoli et al., 2014). Glutamatergic stimulation leads to ERK
70 activation through a NMDAR-mediated calcium-dependent mechanism (Krapivinsky et al., 2003;
71 Mao et al., 2004; Valjent et al., 2005), whereas dopamine differentially regulates ERK activity
72 based on the dopamine receptor subtypes expressed by the neuron (Calabresi et al., 2014).
73 Thus, ERK is hypothesized to initiate appropriate cellular responses to patterned activity from
74 different classes of presynaptic input (Valjent et al., 2005; Girault et al., 2007).

75 Prior work has implicated ERK activity in striatally-mediated locomotor and adaptive
76 behaviors, but these studies have produced conflicting results (Girault et al., 2007; Cerovic et
77 al., 2013; Calabresi et al., 2014). Pharmacological inhibition of ERK signaling prevented

JNeurosci Accepted Manuscript

78 consolidation of motor skill learning, instrumental learning, and habit formation (Bureau et al.,
79 2010; Shiflett et al., 2010; Shiflett and Balleine, 2011). In contrast, loss of ERK1 in germline
80 knockout mice showed surprising effects including baseline hyperactivity, increased synaptic
81 plasticity, enhanced learning, and enhanced locomotor response to cocaine (Selcher et al.,
82 2001; Mazzucchelli et al., 2002; Ferguson et al., 2006; Engel et al., 2009). This disparity has
83 been attributed to increased ERK2 function in ERK1-deleted animals, emphasizing the need to
84 delete both ERK1 and ERK2 in genetic studies (Mazzucchelli et al., 2002; Ferguson et al.,
85 2006). Moreover, prior genetic and pharmacological studies have failed to target ERK inhibition
86 to specific striatal cell types, further confounding interpretations of ERK function. Thus, despite
87 the evidence supporting the importance of ERK signaling to striatal functions and adaptations,
88 pathway specific functions of ERK signaling have not been identified (Fasano and Brambilla,
89 2011).

90 Here, we have delineated cell-type specific functions of ERK signaling by conditionally
91 deleting ERK2 on an ERK1-null background using D1- and D2-Cre lines (Gong et al., 2007).
92 Loss of ERK in D1R-MSNs led to decreased locomotor activity, failure to thrive, and early
93 postnatal lethality, precluding further analysis of the mice. Deletion of ERK in D2R-MSNs
94 resulted in a hyperlocomotor phenotype that is comparable to D2-specific cell ablation studies
95 reported in the literature (Durieux et al., 2009). We report, for the first time, physiological
96 analysis of D2R-MSNs in the setting of complete ERK deletion. ERK-deleted D2R-MSNs are
97 remarkably hypoexcitable, showing reduced frequencies of post-synaptic currents and major
98 reductions in intrinsic excitability. Finally, expression of immediate early and plasticity-
99 associated genes are markedly reduced in ERK-deleted D2R-MSNs both at baseline and in
100 response to pharmacological stimulation. We conclude that ERK signaling is required for
101 pathway specific striatal motor functions. Furthermore, ERK signaling is essential to the
102 excitability and activity-regulated gene expression of D2R-MSNs.
103

JNeurosci Accepted Manuscript

104 **Materials and Methods**

105 *Animals.* Animals were used and maintained in accordance with guidelines published in the NIH
106 *Guide for the Care and Use of Laboratory Animals* and all protocols were approved by the
107 Institutional Animal Care and Use Committee at the University of North Carolina-Chapel Hill.
108 *Drd2*-EGFP, *Drd1a*(EY262)-Cre, *Drd2*(EY43)-Cre, and *Adora2a*-Cre mice were purchased from
109 the Mutant Mouse Regional Resource Center (MMRRC) (Gong et al., 2007). *Erk1*$^{-/-}$ (*Mapk3*$^{-/-}$)
110 and *Erk2*$^{loxP/loxP}$ (*Mapk1*$^{loxP/loxP}$) mice (Nekrasova et al., 2005; Samuels et al., 2008) were kindly
111 provided by G. Landreth (Case Western Reserve University; Cleveland, OH). *Drd1a*^{tdTomato} (Ade
112 et al., 2011), Ai3-EYFP, and Ai9-tdTomato (Madisen et al., 2010) reporter lines were purchased
113 from Jackson Labs (Bar Harbor, ME). All animals were maintained on a C57Bl6/J background.
114 For birth-dating, the day of birth was recorded as postnatal day 0 (P0). All experiments were
115 independently replicated with a minimum of three animals per condition. Power analysis was
116 conducted on preliminary samples to determine sample size using StatMate software
117 (GraphPad, La Jolla, CA). We chose a significance alpha value of 0.05 and a power value of
118 0.8. Mixed-sex samples were utilized for analyses unless otherwise noted. For all experiments,
119 *Erk1*$^{-/-}$;*Erk2* $^{loxP/loxP}$ littermate controls were used for comparison unless otherwise specified. For
120 genotyping, DNA was extracted from tail or toe samples and PCR analysis conducted using
121 standard techniques. Genotyping primer sequences are as follows: *D1-Cre*: Fwd-5'-
122 GCTATGGAGATGCTCCTGATGGAA-3', Rev-5'-CGGCAAACGGACAGAAGCATT-3'; *D2-Cre*:
123 Fwd-5'-GTGCGTCAGCATTTGGAGCAA-3', Rev-5'-CGGCAAACGGACAGAAGCATT-3';
124 *Adora2a-Cre*: Fwd-5'-CGTGAGAAAGCCTTTGGGAAGCT-3', Rev-5'-
125 CGGCAAACGGACAGAAGCATT-3'; *D2-GFP*: Fwd-5'-GAGGAAGCATGCCTTGAAAA-3', Rev-
126 5'-TGGTGCAGATGAACTTCAGG-3'; *ERK1 KO*: Fwd-5'-AAGCAAGGCTAAGCCGTACC-3',
127 Rev (WT)-5'-AAGGTTAACATCCGGTCCAGCA-3', Rev(Mut)-5'-
128 CATGCTCCAGACTGCCTTGG-3'; *ERK2 Flox*: Fwd-5'-AGCCAACAATCCCAAACCTG-3', Rev-
129 5'-GGCTGCAACCATCTCACAAT-3'; *Ai3*: Fwd(WT)-5'-AAGGGAGCTGCAGTGGAGTA-3',

JNeurosci Accepted Manuscript

130 Rev(WT)-5'-CCGAAAATCTGTGGGAAGTC-3', Fwd (Mut)-5'-ACATGGTCCTGCTGGAGTTC-3',
131 Rev(Mut)-5'-GGCATTAAAGCAGCGTATCC-3'; *Ai9*: Fwd(WT)-5'-
132 AAGGGAGCTGCAGTGGAGTA-3; Rev(WT)-5'-CCGAAAATCTGTGGGAAGTC-3', Fwd (Mut)-
133 5'-GGCATTAAAGCAGCGTATCC-3', Rev(Mut)-5'-CTGTTCCTGTACGGCATGG; *D1*^{tdTomato}:
134 Fwd-5'-CTTCTGAGGCGGAAAGAACC-3', Rev-5'-TTTCTGATTGAGAGCATTCG.
135
136 *Acute Tissue Extraction.* Mice were euthanized via cervical dislocation and the brains
137 immediately extracted and rinsed in ice-cold 1x Phosphate Buffered Saline (PBS). The brains
138 were then placed in a chilled acrylic brain matrix (Ted Pella) and 1mm-thick coronal slices were
139 made using a razor blade. Slices were then placed in chilled 1x PBS and, using a 1mm micro
140 punch (Ted Pella), 2-3 tissue punches were extracted from dorsal striatum from each
141 hemisphere for analysis using western blot or gene expression profiling (see below).
142
143 *Western Blotting.* Immediately after extraction, striatal punches were lysed in RIPA buffer
144 (0.05M Tris-HCl, pH 7.4, 0.5M NaCl, 0.25% deoxycholic acid, 1% NP-40, and 1 mM EDTA;
145 Millipore) supplemented with 0.1% SDS, phosphatase inhibitor cocktail II and III (Sigma), and
146 protease inhibitor cocktail (Sigma). After centrifugation, protein concentration was determined
147 from lysates using Bio-Rad protein assay (Bio-Rad) and using BSA as a standard. Equal
148 concentrations of protein were denatured in reducing sample buffer, separated on SDS-Page
149 gel, and then transferred to PVDF membranes (Bio-Rad). After transfer, membranes were
150 blocked with 5% BSA/0.5% Tween-20 in TBS (TBS-T) for 1 hour at room temperature.
151 Membranes were then incubated overnight at 4°C in primary antibody and then rinsed with TBS-
152 T before incubation with HRP-conjugated secondary antibodies in 5% milk/TBS-Tween for 2
153 hours at room temperature. Blots were then washed and detection was performed using a
154 commercially available ECL kit (Pierce). Quantification was conducted using ImageJ software.
155

JNeurosci Accepted Manuscript

156 *Gene Expression Profiling.* Striatal punches were extracted from three littermate control and
157 three mutant P17 male mice generated from three independent litters. Total RNA was extracted
158 using Trizol reagent (Invitrogen) followed by mRNA extraction using an RNeasy Mini Kit
159 (Qiagen) according to manufacturer's instructions. Quantity of extracted mRNA was analyzed
160 using a Nanodrop (ND1000) spectrophotometer and the quality was verified with an Agilent
161 2100 Bioanalyzer. The RNA was then amplified, labeled and hybridized to an Affymetrix
162 Clariom D Array in the UNC Functional Genomics Core using the manufacturer's protocol.
163 Gene Level Differential Expression Analysis was conducted using Transcriptome Analysis
164 Console 3.0 (Affymetrix) using default algorithm parameters for the Clariom D Array. Log_2
165 sample values were used to determine differential gene expression and p-values. Genes were
166 considered upregulated or downregulated if there was a ±1.5 fold difference in expression levels
167 compared to control samples. Changes were considered significant if p-values were ≤0.05. The
168 data discussed in this publication have been deposited in NCBI's Gene Expression Omnibus
169 (Edgar et al., 2002) and are accessible through GEO Series accession number GSE93844
170 (https://www.ncbi.nlm.nih.gov/geo/query/acc.cgi?acc=GSE93844).
171
172 *Tissue Fixation and Preparation.* Mice were anesthetized with a 2.5% Avertin solution (Sigma)
173 and then transcardially perfused with 4% paraformaldehyde/PBS (Sigma). Brains were then
174 post-fixed in 4% paraformaldehyde solution at 4°C overnight. Tissue was mounted in 4% low-
175 melt agarose and 80μm coronal or sagittal sections were generated using a vibratome (Leica).
176
177 *Immunohistochemistry.* Brain sections were rinsed in 1x PBS and then blocked with 5% normal
178 donkey serum/0.1% Triton-100 in 1x PBS (PBS-T) for 1 hour at room temperature. Sections
179 were then incubated in primary antibody in PBS-T for 48 hours at 4°C with slight agitation. After
180 primary incubation, slices were rinsed with PBS-T and then incubated in fluorescent secondary
181 antibodies in PBS-T for 24 hours at 4°C. Sections were again rinsed with PBS-T and then

JNeurosci Accepted Manuscript

182 mounted on Superfrost/Plus slides (Fisher) using Prolong Diamond Mountant (Life
183 Technologies) before coverslipping.
184
185 *Antibodies.* Primary antibodies used for Western blot were rabbit phospho-MAPK1/3(ERK1/2)
186 (Thr202/Tyr204) and rabbit MAPK1/3(ERK1/2) (Cell Signaling Technology). Primary antibodies
187 used for immunohistochemistry were; rabbit Erk2 and rat Ctip2 (1:500,Abcam); rabbit c-FOS
188 (1:500, Cell Signaling Technology), chicken GFP (1:1000,Aves), rabbit RFP and mouse RFP
189 (1:250, Rockland); and rabbit ARC (1:1000, Synaptic Systems). Secondary antibodies used:
190 goat/chicken/donkey Alexa 488, goat/donkey Alexa 568, and goat/donkey Alexa 647 (1:1000;
191 Life Technologies).
192
193 *Viral Injections.* P1 mice were individually cryo-anesthetized on wet ice for 3 min and then
194 immediately injected with 200nl of virus solution using a 5 μl Hamilton syringe fitted with a 32
195 gauge beveled needle mounted to a stereotaxic arm. AAV8-CAG-GFP (UNC Vector Core,
196 Chapel Hill, NC) virus was prepared by diluting concentrated virus with PBS+5% sorbitol+0.1%
197 Fast Green (for visualization) for a final concentration of $5x10^8$ molecules/μl. Unilateral
198 injections were made into the striatum. After the injection, pups were placed on a heating pad
199 until they recovered. Upon recovering, all pups were then placed back into their home cage.
200
201 *Locomotor Activity.* Naïve animals were evaluated for spontaneous locomotor activity using a
202 45cm x 45cm plexiglass arena and Ethovision XT 11.5 (Noldus) video tracking software.
203 Distance traveled was measured using Lowess smoothing to minimize tracking fluctuations. All
204 animals were acclimated to the testing room 3 hours prior to locomotor testing.
205

JNeurosci Accepted Manuscript

206 *Catalepsy.* Two-month old mice were injected with 1mg/kg haloperidol (0.1mg/ml) one hour prior
207 to evaluation of cataleptic behavior. To test catalepsy, both front paws were placed on a
208 horizontal bar mounted 4cm above the testing chamber floor while both hind paws remained on
209 the floor. The time taken to remove both forepaws from the bar, or move both paws sideways on
210 the bar, was recorded. Maximum trial times were 300 seconds. Mice were tested in three
211 consecutive trials unless the maximum cutoff time was achieved in one of the trials. Catalepsy
212 was determined by taking the average of the three trials, or 300 seconds if the maximum was
213 achieved. Haloperidol bromide (Sigma) stock solution was dissolved in (25μl of Glacial Acetic
214 Acid, diluted to 1mg/ml with 0.9% saline, and buffered to pH 6.5 with 1N NaOH). Stock solution
215 was then diluted with 0.9% saline to generate 0.1mg/ml working solution. Injection vehicle
216 solution was generated in the same manner without the addition of haloperidol.
217
218 *Imaging.* All images were acquired using a Zeiss 780 confocal microscope with ZEN 2011
219 software (Carl Zeiss). For comparative studies, image acquisition settings were maintained
220 across all samples. For dendritic spine analysis, five D1R-MSNs and five D2R-MSNs were
221 analyzed per animal from the dorsal striatum. Labelled MSNs were selected randomly for
222 analysis from a group that showed no dendritic overlap with neighboring GFP-labeled cells.
223 Three secondary or tertiary dendrites were then analyzed per cell. For best resolution, only
224 dendrites that were located between 5μm and 20μm from the slice surface and that displayed
225 minimal variation in the horizontal plane were analyzed. All imaged dendrites could be
226 continuously traced back to their respective soma. Three-dimensional 42.5 x 42.5 μm z-stack
227 images of dendritic segments were acquired using 0.388 μm optical sections. After acquisition,
228 images were coded and analysis was conducted by a blinded observer. 3D reconstruction and
229 spine quantification were conducted using Neurolucida 10 software (MBF Bioscience). Dendritic

JNeurosci Accepted Manuscript

230 spines were manually traced throughout each 3D reconstruction image and automatically
231 quantified by the software program.
232
233 *Cell Quantification.* Cell quantification was performed on 637 x 637 μm RGB images acquired
234 from anatomically matched slices of dorsal striatum. All image analysis was conducted by an
235 observer blind to sample genotypes using Photoshop CS3 software (Adobe). The $D1^{tdTomato}$
236 fluorescent reporter was used to identify D1R-MSNs (red fluorescence) and D2R-MSNs (no
237 fluorescence). For each image, all CTIP2-positive MSNs were counted. For the assessment of
238 c-FOS and ARC expressing cells, individual MSNs were first selected based upon Ctip2 (blue
239 channel) labeling using the "quick selection tool". Next, each selected cell was then categorized
240 as a D1R- or D2R-MSN based upon whether it expressed $D1^{tdTomato}$ fluorescence (red channel).
241 Lastly, c-FOS or ARC (green channel) was selected and the integrated pixel intensity and area
242 for each cell was automatically recorded by the software. The average pixel density (pixel
243 intensity/area) was calculated for each selected cell. A cell was considered positive for c-FOS or
244 ARC expression if the average pixel density was greater than 2-fold higher than background.
245 The assessment of ERK2 expression was performed similarly except that ERK2 expression was
246 determined manually by the observer. For analysis of D2GFP-A2aCre;Ai9 experiments, the
247 number of D2GFP, A2aCre;Ai9 and co-labeled cells were manually counted using the count tool
248 in Photoshop.
249
250 *Patch Clamp Electrophysiology.* For all electrophysiology analyses, the experimenter was blind
251 to sample genotypes. Mice were anesthetized with pentobarbital and transcardial perfusions
252 were performed using an ice-cold sucrose cutting solution (0-1°C) containing the following (in
253 mM): 225 sucrose, 119 NaCl, 1.0 NaH_2P0_4, 4.9 $MgCl_2$, 0.1 $CaCl_2$, 26.2 $NaHCO_3$, 1.25 glucose,
254 305-308mOsm). Brains were then removed and submerged in the cutting solution, while coronal
255 sections 300μm thick were then taken using a vibrating blade (Leica, VT 1200). Slices were

JNeurosci Accepted Manuscript

256 then placed in warm aCSF (32°C) containing the following (in mM): 119 NaCl, 2.5 KCl, 1.0
257 NaH_2P0_4, 1.3 MgCl, 2.5 $CaCl_2$, 26.2 $NaHCO_3$, 15 glucose, 305 mOsm). After at least one hour
258 of recovery, slices were perfused with warm aCSF (32°C) containing no pharmacology
259 (excitability recordings) or with 0.5μM tetrodotoxin (mEPSC, mIPSC recordings; Sigma-Aldrich).
260 Neurons were visualized using differential interference contrast through an upright 40x water-
261 immersion objective mounted to an upright microscope (Olympus BX51WI). Fluorescent
262 imaging using a mercury lamp (Olympus U-RFL-T) was used to identify td^{Tomato}-positive (D1)
263 versus td^{Tomato}-negative (D2) medium spiny neurons.

264 Synaptic connectivity was measured through mEPSC and mIPSC recordings, obtained
265 using glass electrodes (3–5 MΩ) back-filled with cesium methylsulfonate internal solution
266 containing of the following (in mM): 117 Cs methanesulfonic acid, 20 HEPES, 2.8 NaCl, 5 TEA,
267 2 ATP, 0.2 GTP, pH 7.35, mOsm 280). mEPSCs were obtained by holding neurons at -70mV
268 for 5 minutes, whereas mIPSCs were obtained by holding neurons at +10mV for 5 minutes.
269 Data acquisition for mEPSCs and mIPSCs occurred at 1 kHz sampling rate through a
270 MultiClamp 700B amplifier connected to a Digidata 1440A digitizer (Molecular Devices).

271 Excitability recordings were obtained using glass electrodes (3–5 MΩ) back-filled with a
272 potassium gluconate internal solution containing of the following (in mM): 130 K gluconate, 10
273 KCl, 10 HEPES, 10 EGTA, 2 $MgCl_2$, 2 ATP, 0.2 GTP, 280 mOsm). Intrinsic neuronal excitability
274 was evaluated by depolarizing each neuron using 800ms current steps (0 to 500pA; 50pA
275 steps). Rheobase was also evaluated by depolarizing each neuron in 50ms current steps (0 to
276 1000pA; 10pA steps). Data acquisition for excitability recordings occurred at a 10 kHz sampling
277 rate. Excitability data was analyzed using a threshold analysis (Clampfit 10.3).

278

279 *Statistical Analysis.* All data were analyzed using Prism 6.0 software (GraphPad, La Jolla, CA).
280 Data are presented as mean ± standard error of measurement unless otherwise noted. For
281 direct comparisons, statistical significance was determined using a two-tailed *t*-test with Welch's

JNeurosci Accepted Manuscript

282 correction. For studies requiring ANOVA, methods used for post-hoc analysis to determine
283 statistical significance are mentioned in the text and figure legends.

JNeurosci Accepted Manuscript

284 **Results**

285 **Cell-type specific deletion of ERK in D1R- and D2R-MSNs**

286 ERK/MAPK (ERK) signaling has been proposed to be a key integrator of dopaminergic
287 and glutamatergic input onto medium spiny neurons and a critical modulator of neuronal
288 plasticity (Girault et al., 2007; Fasano and Brambilla, 2011). To understand the functional role of
289 ERK signaling in the striatum, we generated mutant mice in which *Erk1* and *Erk2* genes were
290 deleted in specific populations of MSNs. Both genes require deletion due to functional
291 redundancy between ERK1 and ERK2 (Selcher et al., 2001; Mazzucchelli et al., 2002). In order
292 to accomplish cell-type specific deletion, we crossed *Erk1*$^{-/-}$ *Erk2*$^{loxP/loxP}$ mice (Nekrasova et al.,
293 2005; Samuels et al., 2008) with the well-documented D1- and D2-Cre lines (Gong et al., 2007).
294 The resulting *Erk1*$^{-/-}$*Erk2*$^{loxP/loxP}$:D1Cre (ERK:D1) and *Erk1*$^{-/-}$ *Erk2*$^{loxP/loxP}$:D2Cre (ERK:D2) lines
295 were germline null for ERK1 and lacked ERK2 expression in D1R- and D2R-MSNs,
296 respectively. Littermate *Erk1*$^{-/-}$*Erk2*$^{loxP/loxP}$ mice were also germline null for ERK1 and were
297 used as controls for all studies unless otherwise noted. As both D1- and D2- receptors are
298 expressed in other brain regions (Gong et al., 2007), we cannot fully exclude the possibility of
299 non-striatal contributions to the strong phenotypes we describe below .

300 To verify that ERK2 was specifically ablated in D1R- and D2R-MSNs of ERK:D1 and
301 ERK:D2 animals, respectively, we analyzed the cell type-specific expression of ERK2 at P21
302 using immunohistochemistry. To distinguish between MSN-subtypes, both the ERK:D1 and
303 ERK:D2 lines were crossed with the D1^{tdTomato} reporter mouse line (Ade et al., 2011).
304 Expression of tdTomato red fluorescent protein exclusively in D1R-MSNs allowed us to
305 distinguish between D1R-MSNs (red fluorescence) and D2R-MSNs (no fluorescence). In
306 ERK:D1 animals, only 3% of D1R-MSNs expressed ERK2 compared to control littermates (Fig.
307 1A; Welch-corrected $t_{(2.16)}$=84.77, p=0.0001). We observed a similar reduction in ERK2
308 expression in D2R-MSNs of ERK:D2 mutant mice (Fig. 1B; Welch-corrected $t_{(2.95)}$=40.64,

JNeurosci Accepted Manuscript

309 p=0.0001). Our findings demonstrate that ERK-activity is ablated in distinct MSN populations of
310 ERK:D1 and ERK:D2 mutant mice.

311 ERK signaling has previously been implicated in cellular growth and maintenance
312 (Cargnello and Roux, 2011). In order to assess the integrity of the ERK-deficient MSN axonal
313 projections, we crossed ERK:D1 and ERK:D2 mice with the Ai3 reporter line which conditionally
314 expresses eYFP in a Cre-dependent manner (Madisen et al., 2010). D1R-MSN projections to
315 the GPi and SNr appeared intact in ERK:D1 mutant mice compared to littermate controls (Fig.
316 1C,D; P21). Similarly, D2R-MSN projections to the GPe also appeared unaffected in ERK:D2
317 animals (Fig. 1E,F; P21). Moreover, we assessed MSN subtype survival at P21 by comparing
318 the percentages of D1R- and D2R-MSN cells in both ERK:D1 and ERK:D2 mice relative to
319 littermate controls. For ERK:D1 mice (n=3 mice/genotypes), we did not observe a significant
320 difference in the percentage of D1R-MSNs (53.1% ± 1.38 (control) vs. 52.3 % ± 0.94 (ERK:D1),
321 Welch-corrected t(3.52)=0.51, p=0.64) or D2R-MSNs (47.4% ± 0.69 (control) vs. 47.3 % ± 0.57
322 (ERK:D1), Welch-corrected t(3.83)=0.13, p=0.90) compared to control littermates. Similarly, we
323 did not observe any significant changes in the percentage of D1R-MSNs (51.6% ± 0.73 (control)
324 vs. 50.6 % ± 2.53 (ERK:D2), Welch-corrected t(2.34)=0.37, p=0.75) or D2R-MSNs (48.5% ±
325 0.73 (control) vs. 49.4 % ± 2.53 (ERK:D2), Welch-corrected t(2.33)=0.37, p=0.74) in ERK:D2
326 mice relative to littermate controls (n=3 mice/genotype). These results suggest that ERK activity
327 is not necessary for the targeting or maintenance of D1R- or D2R-MSN projections. However,
328 we cannot exclude modest effects on axon branching or synaptogenesis.

329 Both ERK:D1 and ERK:D2 mice were generated in appropriate Mendelian ratios.
330 However, we observed a significant reduction in weight gain between P7 and P19 in ERK:D1
331 mutants compared to littermate controls (Fig 1G**;** repeated-measures ANOVA; main genotype
332 effect, $F_{(1,5)}$= 91.90, p=0.0002; main time effect $F_{(6,30)}$= 494.1, p=0.0001, time x genotype
333 interaction: $F_{(6,30)}$=59.92, p=0.0001) and a significant decrease in survival beginning at three
334 weeks of age (Fig. 1H; Median age of death = 28 days; Gehan-Breslow-Wilcoxon survival test:

JNeurosci Accepted Manuscript

335 $\chi^2_{(1)}$=60.72, p=0.0001). In contrast, ERK:D2 mice survived normally compared to littermate
336 controls (Fig. 1H; Gehan-Breslow-Wilcoxon survival test: $\chi^2_{(1)}$=0.065, p=0.799).
337
338 **ERK signaling is required for pathway-specific regulation of locomotor behavior**
339 Previous studies utilizing genetic cell ablation or optogenetic manipulation have shown
340 that D1R-MSN loss or inhibition dramatically reduces locomotor activity (Drago et al., 1998;
341 Kravitz et al., 2010; Durieux et al., 2012), while ablation or optogenetic silencing of D2R-MSNs
342 increases locomotion (Durieux et al., 2009; Kravitz et al., 2010). To determine whether ERK
343 signaling is essential for pathway-specific locomotor function, we assessed basal locomotor
344 activity in naïve ERK:D1 and ERK:D2 mice using a 30-minute open field assay. Analysis of
345 ERK:D1 mice at P21 showed a significant decrease in activity compared to littermate controls
346 demonstrating that ERK activity in D1R-MSNs is necessary for facilitating locomotor behavior
347 (Fig. 2A,B; Welch-corrected $t_{(10.98)}$=3.80, p=0.003). However, the rapid decline in health of
348 ERK:D1 mutant mice precluded us from pursuing more detailed analyses of this line as we
349 could not properly control for potential secondary health effects on D1R-MSN functions.
350 In contrast, ERK:D2 mutant mice showed a significant increase in total distance traveled
351 compared to littermate controls (Fig. 2C,D; Welch-corrected $t_{(10.8)}$=4.93, p=0.0005). To assess
352 potential sexual dimorphism, we also compared open field activity between male and female
353 ERK:D2 mice but found no significant differences (14.2 m ± 2.08 male vs 15.5 m ± 2.09 female;
354 post hoc Welch-corrected $t_{(7.5)}$=0.42, p=0.68, n=4 male mice, 6 female mice). To investigate
355 whether ERK:D2 mice eventually acclimate to the testing arena and reduce their basal activity,
356 we also analyzed the mice in a 3-hour open field assay. Locomotor activity in control animals
357 steadily decreased throughout the trial. In contrast, ERK:D2 mutant mice maintained a high level
358 of activity throughout the three hour testing period (Fig. 2E; repeated-measures ANOVA: main
359 genotype effect: $F_{(1,9)}$= 31.70, p=0.0003; time x genotype interaction: $F_{(17,153)}$=4.73, p=0.0001).

JNeurosci Accepted Manuscript

360 These results demonstrate that ERK activity is required for the proper function of D2R-MSNs in
361 suppressing locomotor behavior.
362
363 **Reduced dendritic spine formation and activity-induced gene expression in ERK-**
364 **deficient D2R-MSNs.**
365 Pharmacological blockade of ERK activity prevents stimulation-induced dendritic spine
366 formation in *ex vivo* slice systems (Goldin and Segal, 2003; Alonso et al., 2004). However, it is
367 unclear whether ERK is required for spinogenesis during normal striatal development. To
368 determine whether dendritic spines are altered in ERK-deficient D2R-MSNs, we labeled sparse
369 populations of MSNs by injecting an AAV8-CAG-GFP virus unilaterally into the striatum of
370 ERK:D2 and littermate control P1 neonatal animals. We then sacrificed the mice at P21, a
371 period during which active synaptogenesis is occurring in the striatum (Tepper et al., 1998;
372 Goldin and Segal, 2003; Alonso et al., 2004; Kozorovitskiy et al., 2012). AAV8-CAG-GFP
373 brightly labels the entire MSN, including dendritic spines, which were then imaged using 3-
374 dimensional confocal microscopy. To distinguish between D1R- and D2R-MSNs, we
375 backcrossed the ERK:D2 line with the $D1^{tdTomato}$ ($D1^{tdT}$) reporter line which expresses tdTomato
376 red fluorescent protein exclusively in D1R-MSNs (Ade et al., 2011). Therefore, all cells which
377 co-expressed GFP and tdTomato were identified as D1R-MSNs while cells that expressed GFP-
378 only were identified as D2R-MSNs (Fig. 3A).
379 At P21, a significant reduction in the density of spines was observed along dendrites of
380 D2R-MSNs in ERK:D2 mice compared to littermate controls (Fig. 3B,C; Welch-corrected
381 $t_{(2.148)}$=6.190, p=0.0211). The effect was more prominent for thinner spines normally associated
382 with plasticity than for thicker, broader spines. Interestingly, we did not observe a significant
383 change in spine density along dendrites of D1R-MSNs in ERK:D2 animals (Fig. 3B,C; Welch-
384 corrected $t_{(2.444)}$=0.5122, p=0.6511).

JNeurosci Accepted Manuscript

385 In addition to changes in dendritic spines, we also observed a reduction in soma size in
386 ERK-deficient MSNs. Quantitative analysis demonstrated that D2R-MSNs showed a significant
387 reduction in somal area in ERK:D2 animals compared to littermate control mice (Control=138.1
388 μm^2 ± 1.855; ERK:D2=113.6 μm^2 ± 2.034; Welch-corrected $t_{(5.95)}$=8.893, p=0.0001; n=4
389 mice/genotype, 5 cells/mouse). These results are consistent with previous reports of reduced
390 soma diameter in D2R-MSNs of conditional BDNF-TrkB knockout mice (Li et al., 2012).
391 Defects in spinogenesis might be expected to lead to reductions in activity regulated
392 transcripts and in abnormal physiological function (see below). To investigate the transcriptional
393 changes that occur in ERK-deleted D2R-MSNs during the period of active striatal
394 synaptogenesis, we performed microarray analysis on striatal punches from littermate control
395 and ERK:D2 mice at P17 (Tepper et al., 1998; Goldin and Segal, 2003; Kozorovitskiy et al.,
396 2012). We observed a significant reduction in the expression of a number of critical immediate
397 early genes (IEGs); *Egr1, Egr2, Egr4, Fosl2, and Srf* levels were all significantly reduced in
398 ERK:D2 mice (Fig. 3D). These reductions are consistent with the idea that ERK-deficient D2-
399 MSNs are severely impaired in their ability to respond to presynaptic stimuli (Okuno, 2011).
400 We also identified a number of genes associated with synapse formation and plasticity
401 that show significantly downregulated expression in ERK:D2 mutant mice (Fig. 3E). We
402 observed significantly reduced expression of the postsynaptic genes *Arc, Homer1, and Nptx2;*
403 the G-protein signaling regulator *Rgs2,* and the transcriptional activator *Nr4a1* (West and
404 Greenberg, 2011; Chen et al., 2014). Taken together, our results related to spinogenesis and
405 activity regulated gene expression suggest that ERK-activity is necessary for proper synaptic
406 function and downstream signaling events.
407
408 **Reduced synaptic drive and intrinsic excitability in ERK-deleted D2R-MSNs**
409 Our findings that ERK:D2 mice have increased locomotor activity logically raise the
410 question of whether electrophysiological properties of D2R-MSNs may also be affected. To test

JNeurosci Accepted Manuscript

411 this, patch-clamp electrophysiological recordings were obtained *ex vivo* to identify the strength
412 of excitatory and inhibitory synaptic input to D2R-MSNs in ERK:D2 and control littermates (Fig.
413 4A). Recordings of miniature excitatory postsynaptic currents (mEPSCs; Fig. 4B,C) revealed a
414 reduction in the frequency ($t_{(16)}$=3.32; p=0.004), but not amplitude ($t_{(16)}$=1.74; p=0.101), of D2R-
415 MSN mEPSCs in ERK:D2 mutant (black trace) versus control mice (grey trace). Recordings of
416 miniature inhibitory postsynaptic currents (mIPSCs; Fig. 4D,E) revealed a reduction in both
417 frequency ($t_{(15)}$=3.13; p=0.007) and amplitude ($t_{(15)}$=3.10; p=0.007) of D2R-MSN mIPSCs in
418 ERK:D2 mice (black trace) versus control mice (grey trace). Taken together, these data reveal a
419 reduction in both excitatory and inhibitory synaptic drive onto D2R-MSNs in ERK:D2 mice.

420 Next, we obtained *ex vivo* patch-clamp electrophysiological recordings to identify the
421 strength of excitatory and inhibitory synaptic input to D1R-MSNs (Fig. 4F) in ERK:D2 mutant
422 and control animals. Recordings of mEPSCs (Fig. 4G,H) revealed no change in the frequency
423 ($t_{(13)}$=1.43; p=0.178) or amplitude ($t_{(13)}$=0.95; p=0.359) of D1R-MSN mEPSCs in ERK:D2 mice
424 (black trace) versus control mice (red trace). Similarly, recordings of miniature inhibitory
425 synaptic currents (mIPSCs; Fig. 4I,J) revealed no change in the frequency ($t_{(13)}$=1.97; p=0.070)
426 or amplitude ($t_{(13)}$=1.18; p=0.260) of D1R-MSN mIPSCs in ERK:D2 mice (black trace) versus
427 control mice (red trace). These results suggest that loss of ERK activity in D2R-MSNs does not
428 significantly alter synaptic drive in D1R-MSNs.

429 In addition to changes in synaptic activity, alterations in the intrinsic excitability of
430 neurons can lead to modifications in the activity of neural networks. Therefore, we evaluated the
431 intrinsic excitability of D2R-MSNs in ERK:D2 and control mice. Overall, we found that the
432 intrinsic excitability of D2R-MSNs in ERK:D2 mice (black trace) was reduced compared to
433 control mice (grey trace) (Fig. 4K,L). Two-way ANOVA revealed a significant interaction ($F_{(10,170)}$
434 = 4.417, p=0.0001), and planned comparisons revealed that the maximum number of action
435 potentials for any sweep was lower in neurons from ERK:D2 mice versus control mice (Table 1).
436 Furthermore, this reduction in action potential frequency in ERK:D2 mice was likely attributable

JNeurosci Accepted Manuscript

437 to a reduced capacity to initiate action potentials, as both rheobase and action potential
438 amplitude were reduced (Table 1). Finally, we performed intrinsic excitability recordings in D1R-
439 MSNs from ERK:D2 and control mice. Overall, we found that the intrinsic excitability of D1R-
440 MSNs in ERK:D2 mice (black trace) was slightly reduced as compared to that of control mice
441 (red trace) (Fig. 4M,N). Two-way ANOVA revealed a significant interaction ($F_{(10,160)}$ =2.93;
442 p=0.002), although planned comparisons revealed no differences in the maximum number of
443 action potentials for any sweep, rheobase, or action potential amplitude (Table 1). These data
444 demonstrate that ERK-deficient D2R-MSNs have a significantly reduced capacity to fire action
445 potentials.
446
447 **Activity regulated gene expression is strongly suppressed in ERK-deleted D2R-MSNs**
448 In D2R-MSNs, dopamine binding to D2R/$G_{\alpha i}$-coupled receptors represses neuronal
449 excitability (Surmeier et al., 2007), while D2R antagonists, including haloperidol, de-repress the
450 cell and allow it to respond to excitatory input (Bonito-Oliva et al., 2011). In mice, haloperidol
451 administration has been shown to induce catalepsy (Sanberg, 1980; Farde et al., 1992), an
452 effect associated with increased phosphorylated ERK activity in D2R-MSNs (Bertran-Gonzalez
453 et al., 2008). To determine if D2R-MSN-specific ERK activity is necessary for cataleptic
454 behavior, we administered haloperidol (1mg/kg I.P.) or vehicle to adult ERK:D2 mutants and
455 littermate controls and tested for cataleptic response one hour after administration using the
456 horizontal bar test (Fig. 5A). Two-way ANOVA revealed a significant difference between
457 genotypes ($F_{(1,24)}$=149.0, p=0.0001), treatment ($F_{(1,24)}$=118.9, p=0.0001), and genotype x
458 treatment interaction ($F_{(1,24)}$=114.3, p=0.0001). Haloperidol administration led to an extended
459 cataleptic freezing response in control mice compared to vehicle treated controls (Fig. 5B;
460 vehicle control vs haloperidol control Tukey's *post-hoc* adjusted: p=0.0001). Strikingly,
461 haloperidol-treated ERK:D2 littermates were insensitive to these cataleptic effects (Fig. 5B;
462 haloperidol control vs. haloperidol ERK:D2 Tukey's *post-hoc* adjusted: p=0.0001). These

JNeurosci Accepted Manuscript

463 findings demonstrate that ERK activity in D2R-MSNs is necessary for the induction of
464 haloperidol-induced catalepsy in mice.

465 In addition to cataleptic behavior, haloperidol administration has also been demonstrated
466 to strongly enhance activity-regulated gene expression in the striatum (Robertson et al., 1992).
467 c-FOS is a well-documented activity-induced gene and has been shown to be selectively
468 upregulated in D2R-MSNs following acute haloperidol administration (Bertran-Gonzalez et al.,
469 2008). We therefore analyzed cell-specific c-FOS expression in ERK-deleted and control D2R-
470 MSNs following haloperidol or vehicle administration. To distinguish between D1R- and D2R-
471 MSNs, we again utilized the $D1^{tdT}$ mouse line to identify D1R-MSNs (see above). We also co-
472 labeled with the ubiquitous MSN marker CTIP2 to exclude non-MSN cells from analysis (Arlotta
473 et al., 2008). CTIP2-positive neurons which expressed tdTomato were identified as D1R-MSNs
474 while CTIP2-positive, tdTomato-negative cells were identified as D2R-MSNs. Two-way ANOVA
475 revealed significant differences between genotype ($F_{(1,8)}$= 1128.7, p=0.0001), treatment ($F_{(1,8)}$=
476 1334.9, p=0.0001), and genotype x treatment interaction ($F_{(1,8)}$= 5220.2, p=0.0001). In control
477 animals, haloperidol treatment significantly increased the percentage of D2R-MSNs expressing
478 c-FOS compared to vehicle treatment (Fig. 5C,E, Tukey's *post-hoc* adjusted: p=0.0001). Fig. 5C
479 shows numerous c-FOS expressing cells in a haloperidol-treated control animal (Upper inset
480 shows high magnification of all 3 labels with yellow arrows indicating D2R-MSNs expressing c-
481 FOS; Lower inset shows c-FOS only). Strikingly, haloperidol administration failed to induce c-
482 FOS expression in D2R-MSNs from ERK:D2 mutants as we found virtually no c-FOS labeling in
483 these mice (Fig. 5 D,E; Tukey's *post-hoc* adjusted: p=0.0001). We did not observe any changes
484 in c-FOS expression in D1R-MSNs in any sample group (Fig. 5F). These findings demonstrate
485 that activity-induced expression of c-FOS is almost completely abolished in ERK-deficient D2R-
486 MSNs.

487 Our observation that activity-induced c-FOS expression is decreased in ERK:D2 mice
488 led us to ask whether activity regulated synaptic plasticity genes were similarly affected. Thus,

JNeurosci Accepted Manuscript

489 we analyzed expression of the activity-induced synaptic cytoskeletal protein ARC in response to
490 haloperidol or vehicle administration in ERK:D2 mice and littermate controls. Two-way ANOVA
491 revealed significant differences between genotype ($F_{(1,8)}$= 129.8, p=0.0001), treatment ($F_{(1,8)}$=
492 84.05, p=0.0001), and genotype x treatment interaction ($F_{(1,8)}$= 80.89, p=0.0001). In control
493 animals, haloperidol treatment greatly increased the percentage of D2R-MSNs expressing ARC
494 compared to vehicle treatment (Fig. 5G,I, Tukey's *post-hoc* adjusted: p=0.0001). Fig. 5G shows
495 numerous ARC-expressing cells in a haloperidol-treated control animal (upper inset shows high
496 magnification of all 3 labels with yellow arrows indicating D2R-MSNs expressing ARC; lower
497 inset shows the ARC label only). In contrast, we observed minimal ARC expression in
498 haloperidol-treated ERK:D2 mice (Fig. 5 H,I; Arrows in the upper and lower insets show ARC-
499 deficient D2R-MSNs; Green cells in the lower inset are D1R-MSN's expressing ARC; Tukey's
500 *post-hoc* adjusted: haloperidol-treated ERK:D2 vs control, p=0.0001).

501 Interestingly, we find that there is significantly increased expression of ARC in D1R-
502 MSNs of ERK:D2 mice in both haloperidol and vehicle treated mutants compared to like-treated
503 littermate controls (Fig. 5J). Two-way ANOVA revealed significant differences between
504 genotype ($F_{(1,8)}$= 129.8, p=0.0001), treatment ($F_{(1,8)}$= 84.05, p=0.0001), and genotype x
505 treatment interaction ($F_{(1,8)}$= 80.89, p=0.0001). Although, D1R-MSNs did not show
506 hyperexcitability in acute slices from ERK:D2 mice, it remains plausible the network level
507 homeostatic changes in D1R-MSN activity might account for this result.

508

509 **Discordant effects of ERK-deletion deletion between the D2-Cre and Adora2-Cre line**

510 In the D2-Cre line, Cre is expressed in a population of striatal cholinergic interneurons in
511 addition to D2R-MSNs (Kravitz et al., 2010; Durieux et al., 2011). Therefore, we performed
512 similar experiments in the Adora2a-Cre line (A2a-Cre) which targets D2R-MSNs but not
513 cholinergic interneurons (Durieux et al., 2009). Surprisingly, we found that ERK:A2a mutant
514 mice did not recapitulate the open field hyperlocomotor phenotype observed in ERK:D2 mice.

JNeurosci Accepted Manuscript

515 Total basal locomotor activity was unchanged between ERK:A2a and littermate control mice
516 (Fig. 6A; Welch-corrected $t_{(10.24)}$=0.717, p=0.489). Likewise, the total locomotor activity profile
517 over the entire 1-hour test session did not significantly differ between ERK:A2a and control
518 animals (Fig. 6B; repeated-measures ANOVA; no main genotype effect, $F_{(1,6)}$= 1.137, p=0.327;
519 no time x genotype interaction: $F_{(5,30)}$=0.127, p=0.985).

520 We next investigated whether ERK:A2a mutant mice also differed in their response to
521 haloperidol. We first tested these animals for haloperidol-induced catalepsy. Interestingly,
522 ERK:A2a mutants responded similarly to ERK:D2 mutant mice, showing a significantly
523 decreased cataleptic response to haloperidol administration compared to haloperidol-treated
524 controls (Fig. 6C; Welch-corrected $t_{(6.86)}$=5.73, p=0.0008). Next, we sought to determine if
525 haloperidol induced changes in the expression of activity induced genes c-FOS and ARC in
526 ERK:A2a mutants. Consistent with our findings in ERK:D2 mutants, there is a significant
527 reduction in c-FOS-expressing D2R-MSNs in ERK:A2a mutant mice in response to haloperidol
528 (Fig. 6D-F; Welch-corrected $t_{(3.61)}$=12.65, p=0.0004). Similarly, ARC expression in D2R-MSNs is
529 almost abolished in ERK:A2a mutant mice after haloperidol administration (Fig. 6G-I; Welch-
530 corrected $t_{(3.24)}$=4.21, p=0.021). Thus, evidence from two independent lines demonstrates that
531 ERK is essential to the regulation of activity-induced gene expression in D2R-MSNs.

532

533 **Temporal delay in A2a-Cre mediated ERK deletion**

534 To determine why ERK:D2 and ERK:A2a may differ in their basal locomotor activities,
535 we first verified that ERK2 expression was ablated in D2R-MSNs of ERK:A2a mice.
536 Unexpectedly, we found that a large proportion of D2R-MSNs expressed ERK2 protein at P21
537 (Fig. 7A). At this stage, more than 40% of D2R-MSNs (45.16% ± 3.34) maintained ERK2
538 expression (Fig. 7B). We repeated the analysis at P28 and observed a decrease in ERK2-
539 positive D2R-MSNs; however, approximately 20% (16.89% ± 3.91) of D2R-MSNs still

JNeurosci Accepted Manuscript

540 expressed ERK2 protein at this age (Fig. 7B). In contrast, ERK2 expression was effectively lost
541 at P21 in ERK:D2 D2R-MSNs (see Fig. 1D). These findings suggest that the A2a-Cre mouse
542 line shows temporally delayed elimination of ERK activity in D2R-MSNs compared to the D2-
543 Cre mouse line.

544 The discrepancy between our ERK:D2 and ERK:A2a findings suggests a potential
545 spatiotemporal incongruity in Cre expression between the A2a- and Drd2- BAC lines. To
546 determine whether the Cre transgene is effectively expressed in all D2R-MSNs in the A2a line,
547 we first backcrossed these mice with Ai9 Cre-dependent reporter mice which label all Cre-
548 expressing cells with tdTomato fluorescent protein (Madisen et al., 2010). We then crossed
549 these A2a-Cre; Ai9 mice with D2-GFP BAC transgenic mice which express GFP in all D2R-
550 expressing cells (Gong et al., 2007) (Fig. 7C). The proportion of cells that expressed D2R-only
551 (green), A2a-only (red), or co-expressed both (A2a/D2; yellow) were then quantified at multiple
552 postnatal stages (Fig 7D). At P14, approximately one-third of labeled cells were D2-only
553 (32.02% ± 7.61), one-third were A2a-only (34.51% ± 3.55) and the remaining one-third co-
554 expressed A2a/D2 (33.47% ± 6.52)(Fig. 7D). At P21 we observed an increase in A2a/D2 co-
555 expression, however nearly 25% of cells still did not show A2a-recombination (Fig. 7D; D2-only:
556 26.33% ± 4.88; A2a-only: 12.62% ± 1.21; A2a/D2: 61.05% ± 3.74). By P28, 15% of D2R-
557 expressing cells still had not undergone A2a-Cre mediated recombination (Fig. 7D; D2-only:
558 14.45% ± 5.06; A2a-only: 7.58% ± 1.08; A2a/D2: 77.97% ± 6.13). This result demonstrates that
559 the A2a-Cre mouse line is delayed in inducing genetic recombination in D2R-MSNs during
560 striatal development.

JNeurosci Accepted Manuscript

561 ***Discussion***

562 ***ERK signaling is essential for MSN pathway specific motor functions***

563 The functions of ERK signaling in the striatum have been the focus of numerous
564 investigations due to the hypothesized importance of the pathway in normal striatal functions
565 and in disease states (Fasano and Brambilla, 2011; Cerovic et al., 2013). Here we present the
566 first genetic evidence that cell-type specific elimination of ERK activity markedly impairs striatal
567 pathway specific motor functions. The severity of these phenotypes presumably reflects the fact
568 that multiple external stimuli (including neurotransmitters and growth factors) and intrinsic neural
569 activity act via ERK to regulate MSN functions.

570 Deletion of both ERK1 and ERK2 in D2R-MSNs results in a pronounced and long-lasting
571 hyperlocomotor phenotype. The intensity of this phenotype was unexpected given that: 1)
572 germline ERK1-KO mice show molecular and behavioral phenotypes indicative of increased
573 neuronal activity and 2) ERK2-hypomorphic mice fail to show locomotor defects (Selcher et al.,
574 2001; Mazzucchelli et al., 2002; Ferguson et al., 2006; Satoh et al., 2007; Engel et al., 2009).
575 However, our results are entirely consistent with studies showing that specific ablation of D2R-
576 MSNs leads to marked hyperlocomotor activity (Saito et al., 2001; Sano et al., 2003; Durieux et
577 al., 2009). ERK:D2 mice are also insensitive to the cataleptic effects of haloperidol, a response
578 mediated by D2R-MSNs (Sanberg, 1980; Farde et al., 1992). This insensitivity to haloperidol is
579 also consistent with results obtained using genetic ablation of D2R-MSNs (Durieux et al., 2012).

580 Given that ERK:D2 mice show no evidence of cell death in the striatum, and that D2R-
581 MSN axonal projections are appropriately targeted and maintained, our data suggest that the
582 behavioral phenotypes observed are a result of dramatically reduced functionality of D2R-
583 MSNs. The hypolocomotive phenotype in ERK:D1 mice also recapitulates D1R-MSN ablation
584 suggesting that ERK activity is necessary for the proper function of both MSN populations
585 (Drago et al., 1998; Durieux et al., 2012; Revy et al., 2014).

JNeurosci Accepted Manuscript

586 The dramatic decline in health and early lethality of ERK:D1 mice precluded a full
587 analysis of this line. The changes in bodyweight and movement after the first postnatal week are
588 consistent with previous findings in both dopamine-deficient mice and knockout models utilizing
589 D1-Cre (Zhou and Palmiter, 1995; Kozorovitskiy et al., 2012). Presumably, ERK:D1 pups cannot
590 acquire nourishment during and after weaning.
591
592 ***ERK-activity is required for D2R-MSN excitability.***
593 ERK:D2 mice exhibit a significantly reduced density of dendritic spines on D2R-MSNs.
594 Previous studies using genetic ERK models did not observe spine alterations (Satoh et al.,
595 2007). Further, D2R-specific knockouts of BDNF-TrkB, an upstream activator of ERK, failed to
596 induce spine changes (Lobo et al., 2010; Besusso et al., 2013). Coincidently, these BDNF-TrkB
597 models also fail to show locomotor changes until at least 1 year of age (Besusso et al., 2013).
598 Thus, loss of ERK in D2R-MSNs leads to more striking defects in spinogenesis, as well as more
599 dramatic changes in locomotion, than does loss of BDNF/TrkB.
600 Changes in dendritic spine density are known to be associated with changes in mEPSCs
601 (Segal, 2005). Consistent with this idea, D2R-MSNs from ERK:D2 mice exhibited a marked
602 reduction in the frequency of mEPSCs. These data suggest reduced excitatory synaptic
603 connectivity in D2R-MSNs. However, we cannot exclude that changes in presynaptic release
604 are also involved. This striking change in synaptic efficacy has the potential to disrupt patterned
605 activity derived from cortical and thalamic excitatory input onto D2R striatal neurons. The
606 observed reduction in frequency and amplitude of mIPSCs would have the potential to further
607 disrupt D2R-MSN circuit functions.
608 In addition to reduced synaptic strength, we observed a dramatic reduction in the
609 intrinsic excitability of ERK-deficient D2R-MSNs. Mechanisms that might explain this phenotype
610 include loss of ERK-mediated phosphorylation of metabotropic or ionotropic receptors, or
611 voltage gated ion channels (Sweatt, 2004). For example, ERK phosphorylation regulates

JNeurosci Accepted Manuscript

612 dendritic localization of the voltage-gated potassium channel Kv4.2, which is abundantly
613 expressed in D2R-MSNs and serves to dampen neuronal excitability (Adams et al., 2000; Yuan
614 et al., 2002; Day et al., 2008). Loss of ERK might lead to increased surface expression of Kv4.2
615 and decreased neuronal excitability. Interestingly, in a recent study of P14 excitatory cortical
616 pyramidal neurons, conditional ERK deletion resulted in hyperexcitability (Xing et al., 2016).
617 Whether these distinct effects on excitability represent differences in ERK regulation in
618 excitatory versus inhibitory neurons or differences in the developmental stages studied is
619 unclear at present.

620 Regardless of mechanisms, the reductions of synaptic efficacy and neuronal excitability
621 observed in D2R-MSNs would likely impair the functioning of D2R-MSNs in governing motor
622 behavior. These effects on excitability may well explain the marked hyperlocomotor activity that
623 we observe in ERK:D2 mice. Furthermore these changes are potentially relevant to a number of
624 pathological states. For example, if similar ERK regulation of excitability occurs in D1R-MSNs, it
625 would be relevant to L-Dopa induced dyskinesia which is known to be associated with striking
626 increases in ERK activity (Gerfen et al., 2002; Feyder et al., 2011). We note that that there may
627 be differences in ERK regulation between D1R- and D2R-MSNs. Indeed, it has been shown that
628 the PKA-dependent phosphorylation of histone H3 in response to cell stimulation is ERK-
629 dependent in D1R-MSNs but ERK-independent in D2R-MSNs (Bertran-Gonzalez et al., 2009).
630

631 ***Expression of activity regulated genes***

632 Previous pharmacological and genetic studies investigating ERK involvement in striatal
633 activity-induced gene expression produced conflicting results. For instance, pan-striatal
634 pharmacological blockade of ERK activity reduced activity-induced gene expression in the
635 striatum (Sgambato et al., 1998; Vanhoutte et al., 1999; Zanassi et al., 2001) whereas germline
636 ERK1 knockout mice showed increased IEG expression in the striatum (Mazzucchelli et al.,
637 2002; Ferguson et al., 2006). Our cell-type specific ablation of ERK activity in D2R-MSNs clearly

JNeurosci Accepted Manuscript

638 demonstrate a strong reduction of activity-regulated gene expression in D2R-MSNs. Gene
639 expression profiling at P17 showed markedly reduced expression of IEGs and synaptic plasticity
640 genes in ERK:D2 mutant mice. We extended these observations using haloperidol
641 administration which normally elicits strong activity-induced expression of these genes (Bertran-
642 Gonzalez et al., 2008). Even upon stimulation with haloperidol, IEG gene expression was
643 largely abrogated in D2R-MSNs. Thus, our data demonstrate that ERK is critical for activity-
644 induced gene expression in MSNs *in vivo*, a process that is essential for driving neuronal
645 synaptic plasticity and adaptations in basal ganglia circuits (Flavell and Greenberg, 2008; West
646 and Greenberg, 2011).

647 ERK is thought to control activity mediated gene expression via activation of a number of
648 critical transcription factors (Girault et al., 2007). However, in ERK-deficient D2R MSNs, it
649 remains unclear whether the reduction in activity-induced gene expression is a direct effect of
650 ERK pathway transcriptional regulation, or whether the reduced neuronal excitability in the ERK
651 deleted MSNs also plays a role. ERK deficiency may also impair translation of local mRNA
652 stores in response to stimuli (O'Donnell et al., 2012). Finally, effects of ERK deficiency could be
653 due to regulation of developmental events (see below). Future studies that inducibly ablate ERK
654 activity will be important in further defining ERK-dependent mechanisms in adult MSNs.

655

656 ***Differences in phenotypes between Adora2a- and D2-Cre ERK-deficient mice***

657 Our studies show a concordance of phenotypes between ERK:D2 mice and ERK:A2a
658 mice in regard to their resistance to haloperidol-induced catalepsy and loss of activity-induced
659 gene expression. A surprising result is that ERK:A2a mice do not exhibit the hyperlocomotor
660 phenotype seen in the ERK:D2 mouse line. A possible explanation is related to different
661 patterns of recombination between the D2- and A2a-Cre mouse lines. While D2-Cre mice target
662 a small population of cholinergic interneurons in the striatum, A2a-Cre transgenic mice
663 reportedly do not target the cholinergic population (Durieux et al., 2009; Kozorovitskiy et al.,

JNeurosci Accepted Manuscript

664 2012; Kharkwal et al., 2016). However, preservation of ERK in cholinergic neurons in the A2a-
665 line is unlikely to account for the behavioral difference as cholinergic interneurons ultimately act
666 on the MSN population. For example, a recent study showed that haloperidol-induced changes
667 in cholinergic neuron activity were directly relayed to D2R-MSNs to mediate cataleptic effects
668 (Kharkwal et al., 2016).

669 A more likely explanation for the different observed behaviors is the temporal delay in
670 Cre-mediated ERK2 deletion in the ERK:A2a mice. At P21, nearly 45% of D2R-MNS continue to
671 express ERK2 in ERK:A2a mice compared to only 3% in ERK:D2 mutants. Even at P28, almost
672 20% of D2R-MSNs still express ERK in A2a-Cre mice. These findings argue that loss of ERK
673 activity specifically in D2R-MSNs before or during the "critical period" of network formation
674 (Tepper et al., 1998; Kozorovitskiy et al., 2012) results in hyperlocomotor behavior, while loss
675 following the critical period results in a milder phenotype. Thus, reductions in ERK/MAP activity
676 before or during the critical period may lead to long lasting modifications of circuit function and
677 behavioral abnormalities. This concept may be pertinent to the etiology of developmental
678 hyperkinetic disorders such as attention deficit hyperactivity disorder (Faraone et al., 2015;
679 Rosenberg et al., 2016). The observation that ERK:A2a mice, which exhibit delayed
680 recombination, show impaired expression of activity regulated genes in response to haloperidol
681 in adulthood underscores the importance of ERK functions in neural plasticity even beyond the
682 critical period.

JNeurosci Accepted Manuscript

683 **Citations**

684 Adams JP, Anderson AE, Varga AW, Dineley KT, Cook RG, Pfaffinger PJ, Sweatt JD (2000)
685 The A-Type Potassium Channel Kv4.2 Is a Substrate for the Mitogen-Activated Protein
686 Kinase ERK. J Neurochem 75:2277-2287.

687 Ade K, Wan Y, Chen M, Gloss B, Calakos N (2011) An Improved BAC Transgenic Fluorescent
688 Reporter Line for Sensitive and Specific Identification of Striatonigral Medium Spiny
689 Neurons. Front Syst Neurosci 5:32.

690 Alonso M, Medina JH, Pozzo-Miller L (2004) ERK1/2 activation is necessary for BDNF to
691 increase dendritic spine density in hippocampal CA1 pyramidal neurons. Learn Mem
692 11:172-178.

693 Arlotta P, Molyneaux BJ, Jabaudon D, Yoshida Y, Macklis JD (2008) Ctip2 controls the
694 differentiation of medium spiny neurons and the establishment of the cellular architecture
695 of the striatum. J Neurosci 28:622-632.

696 Bertran-Gonzalez J, Bosch C, Maroteaux M, Matamales M, Herve D, Valjent E, Girault JA
697 (2008) Opposing patterns of signaling activation in dopamine D1 and D2 receptor-
698 expressing striatal neurons in response to cocaine and haloperidol. J Neurosci 28:5671-
699 5685.

700 Bertran-Gonzalez J, Hakansson K, Borgkvist A, Irinopoulou T, Brami-Cherrier K, Usiello A,
701 Greengard P, Herve D, Girault JA, Valjent E, Fisone G (2009) Histone H3
702 phosphorylation is under the opposite tonic control of dopamine D2 and adenosine A2A
703 receptors in striatopallidal neurons. Neuropsychopharmacology 34:1710-1720.

704 Besusso D, Geibel M, Kramer D, Schneider T, Pendolino V, Picconi B, Calabresi P, Bannerman
705 DM, Minichiello L (2013) BDNF–TrkB signaling in striatopallidal neurons controls
706 inhibition of locomotor behavior. Nat Commun 4:2031.

707 Bonito-Oliva A, Feyder M, Fisone G (2011) Deciphering the Actions of Antiparkinsonian and
708 Antipsychotic Drugs on cAMP/DARPP-32 Signaling. Front Neuroanat 5:38.

JNeurosci Accepted Manuscript

709 Bureau G, Carrier M, Lebel M, Cyr M (2010) Intrastriatal inhibition of extracellular signal-
710 regulated kinases impaired the consolidation phase of motor skill learning. Neurobiol
711 Learn Mem 94:107-115.
712 Calabresi P, Picconi B, Tozzi A, Ghiglieri V, Di Filippo M (2014) Direct and indirect pathways of
713 basal ganglia: a critical reappraisal. Nat Neurosci 17:1022-1030.
714 Cargnello M, Roux PP (2011) Activation and Function of the MAPKs and Their Substrates, the
715 MAPK-Activated Protein Kinases. Microbiol Mol Biol Rev 75:50-83.
716 Cerovic M, d'Isa R, Tonini R, Brambilla R (2013) Molecular and cellular mechanisms of
717 dopamine-mediated behavioral plasticity in the striatum. Neurobiol Learn Mem 105:63-
718 80.
719 Chen Y, Wang Y, Ertürk A, Kallop D, Jiang Z, Weimer Robby M, Kaminker J, Sheng M (2014)
720 Activity-Induced Nr4a1 Regulates Spine Density and Distribution Pattern of Excitatory
721 Synapses in Pyramidal Neurons. Neuron 83:431-443.
722 Day M, Wokosin D, Plotkin JL, Tian X, Surmeier DJ (2008) Differential excitability and
723 modulation of striatal medium spiny neuron dendrites. J Neurosci 28:11603-11614.
724 Drago J, Padungchaichot P, Wong JY, Lawrence AJ, McManus JF, Sumarsono SH, Natoli AL,
725 Lakso M, Wreford N, Westphal H, Kola I, Finkelstein DI (1998) Targeted expression of a
726 toxin gene to D1 dopamine receptor neurons by cre-mediated site-specific
727 recombination. J Neurosci 18:9845-9857.
728 Durieux P, Schiffmann S, de Kerchove d'Exaerde A (2011) Targeting Neuronal Populations of
729 the Striatum. Frontiers in Neuroanatomy 5.
730 Durieux PF, Schiffmann SN, de Kerchove d'Exaerde A (2012) Differential regulation of motor
731 control and response to dopaminergic drugs by D1R and D2R neurons in distinct dorsal
732 striatum subregions. EMBO J 31:640-653.

JNeurosci Accepted Manuscript

733 Durieux PF, Bearzatto B, Guiducci S, Buch T, Waisman A, Zoli M, Schiffmann SN, de Kerchove
734 d'Exaerde A (2009) D2R striatopallidal neurons inhibit both locomotor and drug reward
735 processes. Nat Neurosci 12:393-395.
736 Edgar R, Domrachev M, Lash AE (2002) Gene Expression Omnibus: NCBI gene expression
737 and hybridization array data repository. Nucleic Acids Res 30:207-210.
738 Engel SR, Creson TK, Hao Y, Shen Y, Maeng S, Nekrasova T, Landreth GE, Manji HK, Chen G
739 (2009) The extracellular signal-regulated kinase pathway contributes to the control of
740 behavioral excitement. Mol Psychiatry 14:448-461.
741 Faraone SV, Asherson P, Banaschewski T, Biederman J, Buitelaar JK, Ramos-Quiroga JA,
742 Rohde LA, Sonuga-Barke EJS, Tannock R, Franke B (2015) Attention-
743 deficit/hyperactivity disorder. Nat Rev Dis Primers 1:15020.
744 Farde L, Nordstrom AL, Wiesel FA, Pauli S, Halldin C, Sedvall G (1992) Positron emission
745 tomographic analysis of central D1 and D2 dopamine receptor occupancy in patients
746 treated with classical neuroleptics and clozapine. Relation to extrapyramidal side effects.
747 Arch Gen Psychiatry 49:538-544.
748 Farrell MS, Pei Y, Wan Y, Yadav PN, Daigle TL, Urban DJ, Lee H-M, Sciaky N, Simmons A,
749 Nonneman RJ, Huang X-P, Hufeisen SJ, Guettier J-M, Moy SS, Wess J, Caron MG,
750 Calakos N, Roth BL (2013) A G[alpha]s DREADD Mouse for Selective Modulation of
751 cAMP Production in Striatopallidal Neurons. Neuropsychopharmacology 38:854-862.
752 Fasano S, Brambilla R (2011) Ras–ERK Signaling in Behavior: Old Questions and New
753 Perspectives. Front Behav Neurosci 5:79.
754 Ferguson SM, Fasano S, Yang P, Brambilla R, Robinson TE (2006) Knockout of ERK1
755 enhances cocaine-evoked immediate early gene expression and behavioral plasticity.
756 Neuropsychopharmacology 31:2660-2668.

JNeurosci Accepted Manuscript

757 Feyder M, Bonito-Oliva A, Fisone G (2011) L-DOPA-Induced Dyskinesia and Abnormal
758 Signaling in Striatal Medium Spiny Neurons: Focus on Dopamine D1 Receptor-Mediated
759 Transmission. Front Behav Neurosci 5:71.
760 Flavell SW, Greenberg ME (2008) Signaling Mechanisms Linking Neuronal Activity to Gene
761 Expression and Plasticity of the Nervous System. Annu Rev Neurosci 31:563-590.
762 Gerfen CR, Miyachi S, Paletzki R, Brown P (2002) D1 dopamine receptor supersensitivity in the
763 dopamine-depleted striatum results from a switch in the regulation of ERK1/2/MAP
764 kinase. J Neurosci 22:5042-5054.
765 Gerfen CR, Engber TM, Mahan LC, Susel Z, Chase TN, Monsma FJ, Jr., Sibley DR (1990) D1
766 and D2 dopamine receptor-regulated gene expression of striatonigral and striatopallidal
767 neurons. Science 250:1429-1432.
768 Girault JA, Valjent E, Caboche J, Herve D (2007) ERK2: a logical AND gate critical for drug-
769 induced plasticity? Curr Opin Pharmacol 7:77-85.
770 Goldin M, Segal M (2003) Protein kinase C and ERK involvement in dendritic spine plasticity in
771 cultured rodent hippocampal neurons. Eur J Neurosci 17:2529-2539.
772 Gong S, Doughty M, Harbaugh CR, Cummins A, Hatten ME, Heintz N, Gerfen CR (2007)
773 Targeting Cre recombinase to specific neuron populations with bacterial artificial
774 chromosome constructs. J Neurosci 27:9817-9823.
775 Graybiel AM, Grafton ST (2015) The striatum: where skills and habits meet. Cold Spring Harb
776 Perspect Biol 7:a021691.
777 Hikida T, Kimura K, Wada N, Funabiki K, Nakanishi S (2010) Distinct roles of synaptic
778 transmission in direct and indirect striatal pathways to reward and aversive behavior.
779 Neuron 66:896-907.
780 Kawaguchi Y, Wilson CJ, Emson PC (1990) Projection subtypes of rat neostriatal matrix cells
781 revealed by intracellular injection of biocytin. J Neurosci 10:3421-3438.

JNeurosci Accepted Manuscript

782 Kharkwal G, Brami-Cherrier K, Lizardi-Ortiz JE, Nelson AB, Ramos M, Del Barrio D, Sulzer D,
783 Kreitzer AC, Borrelli E (2016) Parkinsonism Driven by Antipsychotics Originates from
784 Dopaminergic Control of Striatal Cholinergic Interneurons. Neuron 91:67-78.
785 Kozorovitskiy Y, Saunders A, Johnson CA, Lowell BB, Sabatini BL (2012) Recurrent network
786 activity drives striatal synaptogenesis. Nature 485:646-650.
787 Krapivinsky G, Krapivinsky L, Manasian Y, Ivanov A, Tyzio R, Pellegrino C, Ben-Ari Y, Clapham
788 DE, Medina I (2003) The NMDA receptor is coupled to the ERK pathway by a direct
789 interaction between NR2B and RasGRF1. Neuron 40:775-784.
790 Kravitz AV, Freeze BS, Parker PR, Kay K, Thwin MT, Deisseroth K, Kreitzer AC (2010)
791 Regulation of parkinsonian motor behaviours by optogenetic control of basal ganglia
792 circuitry. Nature 466:622-626.
793 Li Y, Yui D, Luikart BW, McKay RM, Li Y, Rubenstein JL, Parada LF (2012) Conditional ablation
794 of brain-derived neurotrophic factor-TrkB signaling impairs striatal neuron development.
795 Proc Natl Acad Sci U S A 109:15491-15496.
796 Lobo MK, Covington HE, 3rd, Chaudhury D, Friedman AK, Sun H, Damez-Werno D, Dietz DM,
797 Zaman S, Koo JW, Kennedy PJ, Mouzon E, Mogri M, Neve RL, Deisseroth K, Han MH,
798 Nestler EJ (2010) Cell type-specific loss of BDNF signaling mimics optogenetic control of
799 cocaine reward. Science 330:385-390.
800 Madisen L, Zwingman TA, Sunkin SM, Oh SW, Zariwala HA, Gu H, Ng LL, Palmiter RD,
801 Hawrylycz MJ, Jones AR, Lein ES, Zeng H (2010) A robust and high-throughput Cre
802 reporting and characterization system for the whole mouse brain. Nat Neurosci 13:133-
803 140.
804 Mao L, Tang Q, Samdani S, Liu Z, Wang JQ (2004) Regulation of MAPK/ERK phosphorylation
805 via ionotropic glutamate receptors in cultured rat striatal neurons. Eur J Neurosci
806 19:1207-1216.

JNeurosci Accepted Manuscript

807 Mazzucchelli C, Vantaggiato C, Ciamei A, Fasano S, Pakhotin P, Krezel W, Welzl H, Wolfer DP,
808 Pages G, Valverde O, Marowsky A, Porrazzo A, Orban PC, Maldonado R, Ehrengruber
809 MU, Cestari V, Lipp HP, Chapman PF, Pouyssegur J, Brambilla R (2002) Knockout of
810 ERK1 MAP kinase enhances synaptic plasticity in the striatum and facilitates striatal-
811 mediated learning and memory. Neuron 34:807-820.
812 Nekrasova T, Shive C, Gao Y, Kawamura K, Guardia R, Landreth G, Forsthuber TG (2005)
813 ERK1-deficient mice show normal T cell effector function and are highly susceptible to
814 experimental autoimmune encephalomyelitis. J Immunol 175:2374-2380.
815 Nelson AB, Kreitzer AC (2014) Reassessing Models of Basal Ganglia Function and Dysfunction.
816 Annu Rev Neurosci 37:117-135.
817 O'Donnell A, Odrowaz Z, Sharrocks AD (2012) Immediate-early gene activation by the MAPK
818 pathways: what do and don't we know? Biochem Soc Trans 40:58-66.
819 Okuno H (2011) Regulation and function of immediate-early genes in the brain: beyond
820 neuronal activity markers. Neurosci Res 69:175-186.
821 Pascoli V, Cahill E, Bellivier F, Caboche J, Vanhoutte P (2014) Extracellular signal-regulated
822 protein kinases 1 and 2 activation by addictive drugs: a signal toward pathological
823 adaptation. Biol Psychiatry 76:917-926.
824 Revy D, Jaouen F, Salin P, Melon C, Chabbert D, Tafi E, Concetta L, Langa F, Amalric M,
825 Kerkerian-Le Goff L, Marie H, Beurrier C (2014) Cellular and Behavioral Outcomes of
826 Dorsal Striatonigral Neuron Ablation: New Insights into Striatal Functions.
827 Neuropsychopharmacology 39:2662-2672.
828 Robertson GS, Vincent SR, Fibiger HC (1992) D1 and D2 dopamine receptors differentially
829 regulate c-fos expression in striatonigral and striatopallidal neurons. Neuroscience
830 49:285-296.

JNeurosci Accepted Manuscript

831 Rosenberg MD, Finn ES, Scheinost D, Papademetris X, Shen X, Constable RT, Chun MM
832 (2016) A neuromarker of sustained attention from whole-brain functional connectivity.
833 Nat Neurosci 19:165-171.
834 Saito M, Iwawaki T, Taya C, Yonekawa H, Noda M, Inui Y, Mekada E, Kimata Y, Tsuru A,
835 Kohno K (2001) Diphtheria toxin receptor-mediated conditional and targeted cell ablation
836 in transgenic mice. Nat Biotechnol 19:746-750.
837 Samuels IS, Karlo JC, Faruzzi AN, Pickering K, Herrup K, Sweatt JD, Saitta SC, Landreth GE
838 (2008) Deletion of ERK2 Mitogen-Activated Protein Kinase Identifies Its Key Roles in
839 Cortical Neurogenesis and Cognitive Function. J Neurosci 28:6983-6995.
840 Sanberg PR (1980) Haloperidol-induced catalepsy is mediated by postsynaptic dopamine
841 receptors. Nature 284:472-473.
842 Sano H, Yasoshima Y, Matsushita N, Kaneko T, Kohno K, Pastan I, Kobayashi K (2003)
843 Conditional ablation of striatal neuronal types containing dopamine D2 receptor disturbs
844 coordination of basal ganglia function. J Neurosci 23:9078-9088.
845 Satoh Y, Endo S, Ikeda T, Yamada K, Ito M, Kuroki M, Hiramoto T, Imamura O, Kobayashi Y,
846 Watanabe Y, Itohara S, Takishima K (2007) Extracellular signal-regulated kinase 2
847 (ERK2) knockdown mice show deficits in long-term memory; ERK2 has a specific
848 function in learning and memory. J Neurosci 27:10765-10776.
849 Segal M (2005) Dendritic spines and long-term plasticity. Nat Rev Neurosci 6:277-284.
850 Selcher JC, Nekrasova T, Paylor R, Landreth GE, Sweatt JD (2001) Mice Lacking the ERK1
851 Isoform of MAP Kinase Are Unimpaired in Emotional Learning. Learn Mem 8:11-19.
852 Sgambato V, Pagès C, Rogard M, Besson M-J, Caboche J (1998) Extracellular Signal-
853 Regulated Kinase (ERK) Controls Immediate Early Gene Induction on Corticostriatal
854 Stimulation. J Neurosci 18:8814-8825.
855 Shiflett MW, Balleine BW (2011) Contributions of ERK signaling in the striatum to instrumental
856 learning and performance. Behav Brain Res 218:240-247.

JNeurosci Accepted Manuscript

857 Shiflett MW, Brown RA, Balleine BW (2010) Acquisition and Performance of Goal-Directed
858 Instrumental Actions Depends on ERK Signaling in Distinct Regions of Dorsal Striatum
859 in Rats. J Neurosci 30:2951-2959.
860 Surmeier DJ, Ding J, Day M, Wang Z, Shen W (2007) D1 and D2 dopamine-receptor
861 modulation of striatal glutamatergic signaling in striatal medium spiny neurons. Trends
862 Neurosci 30:228-235.
863 Sweatt JD (2004) Mitogen-activated protein kinases in synaptic plasticity and memory. Curr
864 Opin Neurobiol 14:311-317.
865 Tepper JM, Sharpe NA, Koos TZ, Trent F (1998) Postnatal development of the rat neostriatum:
866 electrophysiological, light- and electron-microscopic studies. Dev Neurosci 20:125-145.
867 Thomas GM, Huganir RL (2004) MAPK cascade signalling and synaptic plasticity. Nat Rev
868 Neurosci 5:173-183.
869 Valjent E, Pascoli V, Svenningsson P, Paul S, Enslen H, Corvol JC, Stipanovich A, Caboche J,
870 Lombroso PJ, Nairn AC, Greengard P, Herve D, Girault JA (2005) Regulation of a
871 protein phosphatase cascade allows convergent dopamine and glutamate signals to
872 activate ERK in the striatum. Proc Natl Acad Sci U S A 102:491-496.
873 Vanhoutte P, Barnier J-V, Guibert B, Pagès C, Besson M-J, Hipskind RA, Caboche J (1999)
874 Glutamate Induces Phosphorylation of Elk-1 and CREB, Along with c-fos Activation, via
875 an Extracellular Signal-Regulated Kinase-Dependent Pathway in Brain Slices. Mol Cell
876 Biol 19:136-146.
877 West AE, Greenberg ME (2011) Neuronal Activity–Regulated Gene Transcription in Synapse
878 Development and Cognitive Function. Cold Spring Harb Perspect Biol 3:a005744.
879 Xing L, Larsen RS, Bjorklund GR, Li X, Wu Y, Philpot BD, Snider WD, Newbern JM (2016)
880 Layer specific and general requirements for ERK/MAPK signaling in the developing
881 neocortex. eLife 5:e11123.

JNeurosci Accepted Manuscript

882 Yuan LL, Adams JP, Swank M, Sweatt JD, Johnston D (2002) Protein kinase modulation of
883 dendritic K+ channels in hippocampus involves a mitogen-activated protein kinase
884 pathway. J Neurosci 22:4860-4868.
885 Zanassi P, Paolillo M, Feliciello A, Avvedimento EV, Gallo V, Schinelli S (2001) cAMP-
886 dependent Protein Kinase Induces cAMP-response Element-binding Protein
887 Phosphorylation via an Intracellular Calcium Release/ERK-dependent Pathway in
888 Striatal Neurons. J Biol Chem 276:11487-11495.
889 Zhou QY, Palmiter RD (1995) Dopamine-deficient mice are severely hypoactive, adipsic, and
890 aphagic. Cell 83:1197-1209.
891

JNeurosci Accepted Manuscript

892 **Figure 1. ERK-deficient MSNs show proper targeting of axonal projections.**

893 **A)** Quantification of the relative percentage of ERK2-positive D1R-MSNs in control and ERK:D1
894 mutant mice at P21. ERK2 (green) is co-expressed with $D1^{tdTomato}$ (red) in D1R-MSNs of
895 littermate control mice but is lost in virtually all D1R-MSNs of ERK:D1 mutant mice (*p<0.001;
896 n=3 mice/genotype, 150 cells/mouse) (Scale bar =50μm). **B)** Quantification of the percentage of
897 ERK2-postive D2R-MSNs in littermate control and ERK:D2 mutant mice at P21. ERK2 (green)
898 is expressed in in both $D1^{tdTomato}$- positive D1R-MSNs and $D1^{tdTomato}$-negative D2R-MSNs of
899 littermate control mice but is lost in virtually all $D1^{tdTomato}$-negative D2R-MSNs of ERK:D2 mutant
900 mice (*p<0.001; n=3 mice/genotype, 150 cells/mouse) (Scale bar =50μm). **C-D)** Control ($ERK^{-/-}$
901 ;$ERK2^{wt/wt}$:$D1^{Cre}$) and ERK:D1 mutant mice were backcrossed with Cre-dependent fluorescent
902 reporter Ai3 mice to label all D1R-MSN projections with eYFP. Normal D1R axon targeting to
903 the GPi and SNr is observed in control **(C)** and ERK:D1 mutant **(D)** mice. Scale bar=1mm. **(E-F)**
904 Control ($ERK^{-/-}$;$ERK2^{wt/wt}$:$D2^{Cre}$) and ERK:D2 mutant mice were backcrossed with Ai3 mice to
905 label D2R-MSN axonal projections with eYFP. Normal D2R axon targeting to the GPe is
906 observed in control **(E)** and ERK:D2 mutant **(F)** mice. Insets show magnified images of GPe.
907 Scale bar=1mm. **(G)** Quantification of weight gain during the second and third postnatal weeks
908 in ERK:D1 mutant mice compared to $ERK^{-/-}$;$ERK2^{Fl/Fl}$ littermate controls. ERK:D1 animals show
909 significant deficits in weight gain beginning at P7 and continuing through P19 (n=6
910 animals/genotype, main effect for genotype F (1, 10) = 84.96, *p<0.0001, Bonferroni post-hoc
911 comparison). **(H)** Kaplan-Meier Survival curve of ERK:D1 (blue line, n=80 mice) and ERK:D2
912 (green line; n=71 mice) mice compared to $ERK1^{-/-}$;$ERK2^{Fl/Fl}$ controls (black line, n=57 mice).
913 ERK:D1 mice show a significant reduction in survival (*p<0.0001, Post-Hoc Gehan-Breslow-
914 Wilcoxon test). Abbreviations: eYFP: enhanced yellow fluorescent protein; GPi: Globus Pallidus
915 internae; GPe: Globus Pallidus externae; SNr: Substantia Nigra reticulata. All data presented as
916 mean±SEM.

JNeurosci Accepted Manuscript

917 **Figure 2. ERK signaling is required for pathway specific regulation of locomotor behavior**
918 **A)** Quantification of total distance traveled in a 30 min testing period by ERK:D1 (blue bar) and
919 paired littermate control (grey bar) mice at P21. ERK:D1 animals show a significant reduction in
920 locomotor activity (*p<0.01, n=10 mice/genotype). **B)** Representative recordings of total
921 distance traveled (30 min) in control and ERK:D1 animals. **C)** Quantification of total distance
922 traveled in a 30 min testing period by ERK:D2 mutant mice (green bar) and paired littermate
923 controls (grey bar). ERK:D2 mutants show significantly more locomotor activity than controls
924 (*p<0.001, n=10mice/genotype). **D)** Representative tracks of cumulative open field activity for
925 control and ERK:D2 mutant mice. **E)** 3 hour open field analysis of ERK:D2 mice and controls.
926 Total distance traveled as a function of time. ERK:D2 mutant mice (green trace) show
927 significantly increased movement throughout the entire 3 hour testing period compared to
928 control animals (grey trace) which steadily reduce activity throughout the trial (*p<0.001; n=10
929 mice/genotype). All data reported as Mean ± SEM.

JNeurosci Accepted Manuscript

930 **Figure 3. ERK signaling is required for proper spinogenesis and expression of synaptic**
931 **plasticity genes**
932 **A)** Representative images of D1R- and D2R-MSNs labeled with AAV8-CAG-GFP virus (green).
933 D1R-MSNs are identified by their expression of the $D1^{tdTomato}$ transgene (red) while D2R-MSNs
934 are $D1^{tdTomato}$- negative. GFP-expressing D2R-MSNs appear green whereas GFP-expressing
935 D1R-MSNs appear yellow (Scale bar=20μm). **B)** AAV8-CAG-GFP efficiently labels MSN
936 dendritic spines. D2R-MSNs in ERK:D2 mutant mice show a significant reduction in spine
937 density compared to littermate controls. In contrast, there is no difference in spine density on
938 D1R-MSNs between mutant and control animals (scale bar=5μm). **C)** Quantification of mean
939 spine density shows a reduction in dendritic spines in D2R-MSNs (*$p<0.05$; n=3 mice/genotype,
940 15 dendrites/mouse), but not D1R-MSNs ($p<0.65$; n=3 mice/genotype, 15 dendrites/mouse), in
941 ERK:D2 mutant mice compared to littermate controls. **D-E)** Microarray analysis of P17 striatum
942 (n=3 male mice/genotype) showing dramatic reduction in the expression of activity-induced
943 immediate early genes **(D)** and genes associated with synaptic plasticity **(E)**. *$p<0.05$.

JNeurosci Accepted Manuscript

944 **Figure 4. Markedly reduced excitability of ERK-deleted D2R-MSNs.**

945 **A)** Image of pipette recording from a D2R-MSN which is negative for $D1^{tdTomato}$ (red). **B)**
946 Representative mEPSC recordings of D2R-MSNs from control (grey) and ERK:D2 mutant
947 (black) mice. **C)** Summary of mEPSC frequencies and amplitudes from control (grey; n=3 mice,
948 n=10 neurons) and ERK:D2 mutant (black; n=3 mice, n=8 neurons) D2R-MSNs. mEPSC
949 frequency is significantly reduced in ERK:D2 mutant D2R-MSNs (*p<0.01) while mEPSC
950 amplitude is unchanged. **D)** Representative mIPSC recordings of D2R-MSNs from control (grey)
951 and ERK:D2 mutant (black) mice. **E)** Summary of mIPSC frequencies and amplitudes from
952 control (grey; n=3 mice; n=10 neurons) and ERK:D2 mutant (black; n=3 mice; n=7 neurons)
953 D2R-MSNs. Both mIPSC frequency and amplitude are significantly reduced in ERK:D2 mutant
954 D2-MSNs (*p<0.01). **F)** Representative image of recording pipette in a $D1^{tdTomato}$-positive (red)
955 D1R-MSN. **G)** Representative mEPSC recordings of D1R-MSNs from control (red) and ERK:D2
956 mutant (black) mice. **H)** Summary of mEPSC frequencies and amplitudes from control (red; n=3
957 mice; n=8 neurons) and ERK:D2 mutant (black; n=3 mice; n=7 neurons) D1R-MSNs. There is
958 no significant change in mEPSC frequency or amplitude in ERK:D2 mutant D1R-MSNs
959 compared to control. **I)** Representative mIPSC recordings of D1R-MSNs from control (red) and
960 ERK:D2 mutant (black) mice. **J)** Summary of mIPSC frequencies and amplitudes from control
961 (red; n=3 mice; n=8 neurons) and ERK:D2 mutant (black; n=3 mice; n=7 neurons) D1R-MSNs.
962 There is no significant difference between ERK:D2 mutant D1R- and control MSNs. **K)**
963 Representative traces of whole cell patch clamp recordings from D2R-MSNs in control (grey)
964 and ERK:D2 mutant (black) mice. **L)** Relationship between elicited action potential responses
965 and somatic current injection in D2R-MSNs of control (grey; n=3 mice; n=9 neurons) and
966 ERK:D2 mutant (black; n=3 mice; n=10 neurons) mice. D2R-MSNs from ERK:D2 mutant mice
967 have a significantly reduced capacity to elicit action potentials (*p<0.001). **M)** Representative
968 traces of whole cell patch clamp recordings from D1R-MSNs in control (red) and ERK:D2
969 mutant (black) mice. **N)** Relationship between elicited action potential responses and somatic

JNeurosci Accepted Manuscript

970 current injection in D1R-MSNs of control (red; n=3 mice; n=9 neurons) and ERK:D2 mutant
971 (black; n=3 mice; n=9 neurons) mice. Intrinsic excitability in D1R-MSNs of ERK:D2 mutant mice
972 was slightly, but significantly, reduced compared to controls (*$p<0.01$).

JNeurosci Accepted Manuscript

973 **Figure 5. Activity regulated gene expression is strongly suppressed in ERK-deleted D2R-**
974 **MSNs**
975 **A)** Representative image of cataleptic response to haloperidol using horizontal bar test. **B)**
976 Quantification of cataleptic response (freezing) to haloperidol (1mg/kg) or vehicle in littermate
977 control and ERK:D2 mutant mice. Control mice exhibit a robust cataleptic response to
978 haloperidol compared to vehicle treated controls (*p=0.001, n=7 mice/genotype/condition). The
979 cataleptic response is effectively abolished in the mutant mice (*p=0.001, haloperidol-treated
980 ERK:D2 vs haloperidol treated control; n=7 mice/condition). Vehicle treated mice show no
981 cataleptic response (n=7 mice per genotype per treatment). **C-D)** c-FOS (green) expression in
982 control and ERK:D2 mutant striatum 1 hour after haloperidol administration. CTIP2 (blue)
983 identifies all MSNs; $D1^{tdTomato}$ (red) identifies the D1R-MSN subpopulation. All D2R-MSNs are
984 CTIP2(+);tdTomato(-). Insets; magnified images showing all 3 labels (upper) and c-FOS only
985 (lower) demonstrating that c-FOS is strongly upregulated in D2R-MSNs (yellow arrows) in
986 control **(C)** but not ERK:D2 animals **(D)**. **E)** Quantification of MSN-specific c-FOS expression
987 after haloperidol (1mg/kg) or vehicle administration (*p<0.001; n= 3 mice/genotype; 200-250
988 cells/mouse). **F)** No changes in c-FOS expression are observed in D1R-MSNs in either control
989 or ERK:D2 mutant animals. (n=3 animals/genotype, 200-250 cells/animal). **G-H)** ARC (green)
990 expression in control and ERK:D2 mutant striatum 1 hour after haloperidol administration.
991 CTIP2 (blue) identifies all MSNs; $D1^{tdTomato}$ (red) identifies the D1R-MSN subpopulation. All
992 D2R-MSNs are CTIP2(+);tdTomato(-). Insets: magnified images demonstrating that ARC is
993 upregulated in D2R-MSNs (yellow arrows) in control **(G)** but not ERK:D2 animals **(H)**. **I)**
994 Quantification of D2R-MSN-specific ARC expression after haloperidol (1mg/kg) or vehicle
995 administration (*p<0.001; n= 3 mice/genotype; 200-250 cells/mouse). **J)** D1R-MSNs in ERK:D2
996 mutant mice express significantly more ARC compared to controls regardless of treatment
997 (#p<0.05, *p<0.001; n= 3 mice/genotype; 200-250 cells/mouse). All data presented as Mean ±
998 SEM. Scale bar=50μm; inset =10μm.

JNeurosci Accepted Manuscript

999 **Figure 6. Basal and haloperidol-induced behavioral and gene expression changes in**
1000 **ERK:A2a mice.**
1001 **A-B)** Open field locomotor testing of ERK:A2a and control mice (n=7 animals/genotype). **A)**
1002 There is no significant difference in cumulative distance traveled (1 hour test) between ERK:A2a
1003 mutant and control littermates. **B)** Total distance traveled as a function of time. No differences
1004 are observed between mutant and control animals. **C)** Cataleptic response 1 hour after
1005 haloperidol administration (1mg/kg). ERK:A2a mutant mice have a significantly reduced
1006 cataleptic response compared to littermate controls (*p<0.001; n=6 mice/genotype). **D-E)**
1007 Immunohistochemical labeling of activity-induced gene expression 1 hour after haloperidol
1008 administration. All MSNs are labeled with Ctip2 (blue). D1R-MSNs are distinguished from D2R-
1009 MSNs by their expression of $D1^{tdTomato}$(red). c-FOS (green) is upregulated in D2R-MSNs of
1010 control **(D)** but not ERK:A2a mutant (**E)** mice (Insets show higher magnification of all 3 labels
1011 (upper) and c-FOS only (lower). D2R-MSNs are indicated by yellow arrows). **F)** Quantitative
1012 analysis shows a significant reduction in the percentage of D2R-MSNs expressing c-FOS in
1013 ERK:A2a mutant animals compared to control animals (*p<0.001; n=3 mice/genotype; 200-250
1014 cells/mouse). **G-H)** ARC (green) is upregulated in D2R-MSNs (yellow arrows) in control **(G)** but
1015 not ERK:A2a mutant **(H)** animals. **I)** Quantitative analysis demonstrating a significant decrease
1016 in the percentage of D2R-MSNs which upregulate ARC in ERK:A2a mutant mice (*p<0.05; n= 3
1017 mice/genotype; 200-250 cells/mouse). All data presented as mean ± SEM. Scale bars=50μm
1018 (inset=20μm).

JNeurosci Accepted Manuscript

1019 **Figure 7. Delayed loss of ERK activity in ERK:A2a mice.**

1020 **A)** Representative image of P21 ERK:A2a striatum. CTIP2 (blue) labels all MSNs while D2R-
1021 MSNs are identified as negative for $D1^{tdTomato}$ expression (red). A subpopulation of D2R-MSNs in
1022 ERK:A2a mutants maintain ERK2 expression (green, white arrows). ERK2-deficient D2R-MSNs
1023 are indicated with a white asterisk (scale bar=20μm). **B)** Quantitative analysis of ERK2
1024 expression in P21 and P28 ERK:A2a striatum. Approximately half of all D2R-MSNs maintain
1025 ERK2 expression at P21. By 28, approximately 15% of D2R-MSNs continue to express ERK2.
1026 (n=3 animals/genotype; 500-600cells/animal). **C)** Co-localization of $D2^{GFP}$ (green) and
1027 $A2a^{Cre}$:Ai9 (red) at P14 (scale bar=50μm). **D)** Quantification of $D2^{GFP}$ and $A2a^{Cre}$:Ai9 co-
1028 localization at P14, P21, and P28. Data presented as percentage of total D2R-MSNs counted.
1029 Note that the percentage of D2R-MSNs which express both GFP and Ai9 is low at P14. The
1030 percentage increases over time, but complete recombination in D2R-MSNs is not observed,
1031 even by P28 (n=3 animals/time point; 500-600 cells/animal). All data presented as mean ± SEM.

JNeurosci Accepted Manuscript

1032 **Table 1 – Membrane and Action potential properties of ERK:D2 MSNs**

1033 Basic membrane properties and action potential properties in D2R- (top) and D1R-
1034 (bottom) MSNs, recorded during intrinsic excitability experiments. IR, input resistance;
1035 RMP, resting membrane potential; Rheo, rheobase; Thresh, action potential threshold;
1036 Amp, action potential amplitude; H.W., half-width; MaxAPs, maximum number of action
1037 potentials for any current step. *$p<0.05$ versus control neurons.

JNeurosci Accepted Manuscript

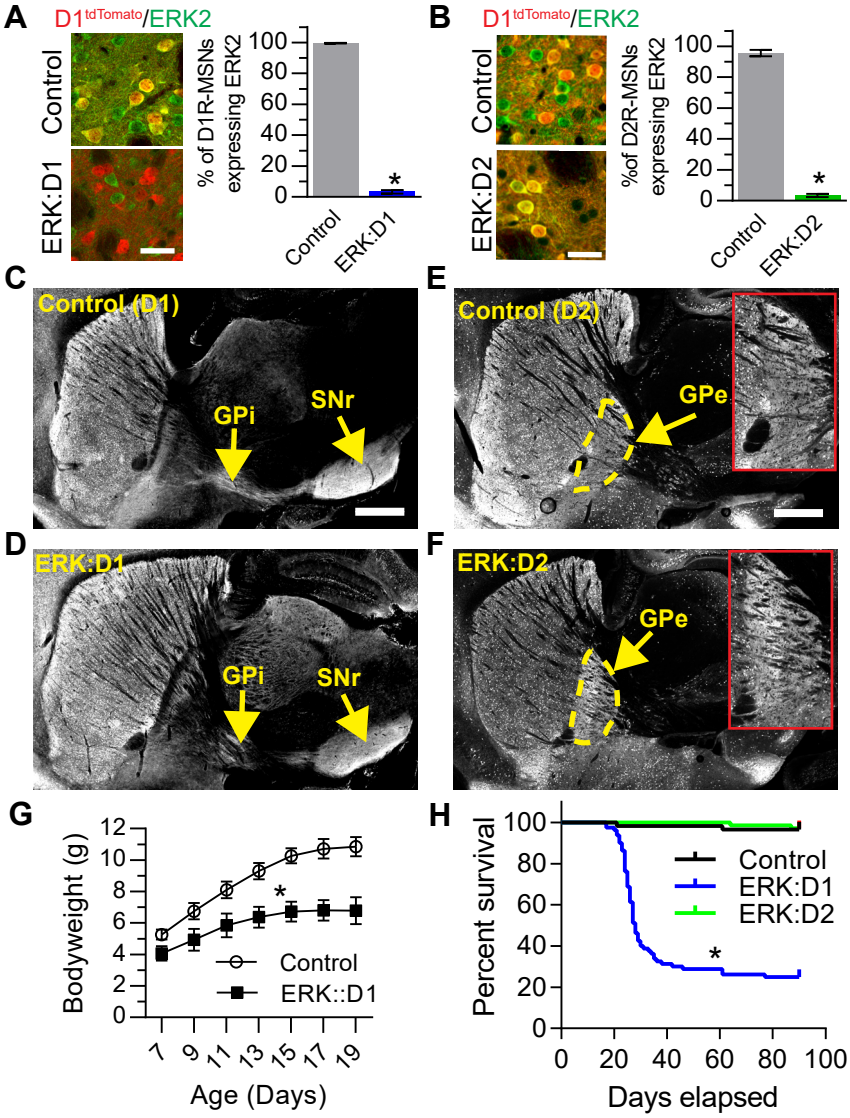

JNeurosci Accepted Manuscript

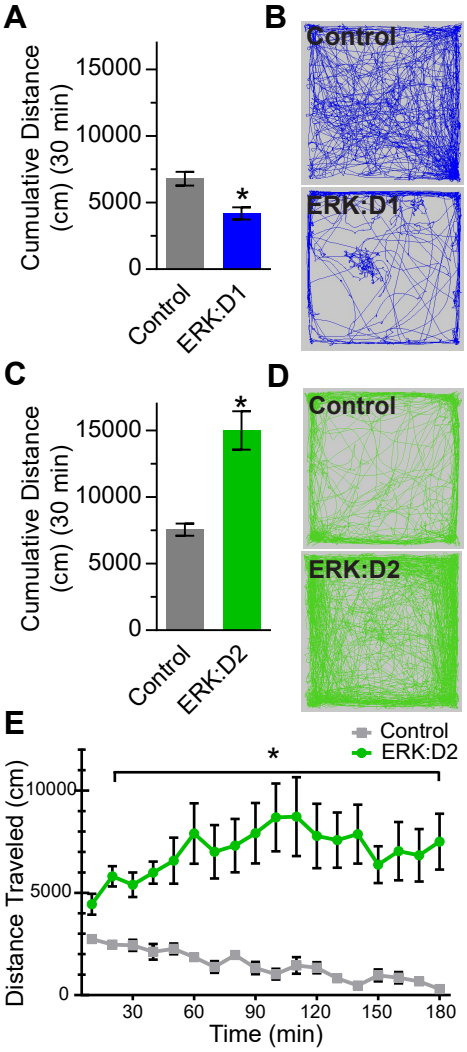

JNeurosci Accepted Manuscript

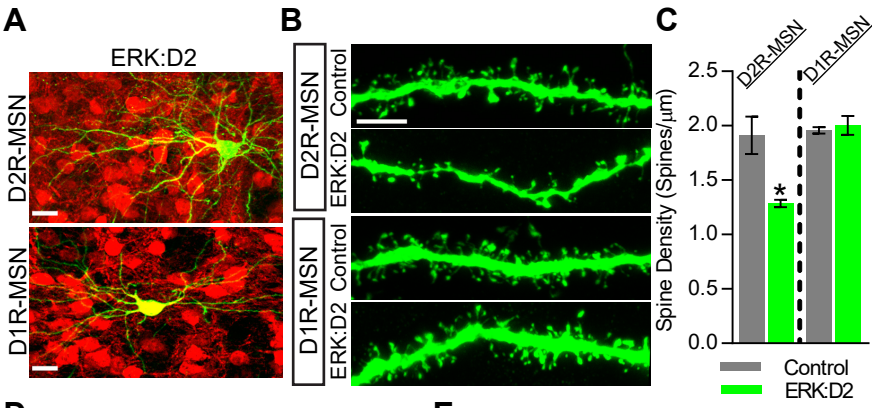

D

Immediate Early Genes

Gene	Anova p-Value	Fold Change (Compared to Control)
Egr1	0.005808	-2.1
Egr2	0.000953	-1.96
Fos	0.079076	-1.91
Fosl2	0.032868	-1.78
Egr3	0.069367	-1.74
Egr4	0.002845	-1.51
Fosb	0.067583	-1.38
Klf10	0.052887	-1.37
Srf	0.011213	-1.36

E

Synaptic Plasticity Associated Genes

Gene	Anova p-Value	Fold Change (Compared to Control)
Arc	0.011947	-2.85
Nr4a1	0.00621	-2.44
Rgs2	0.001251	-1.72
Homer1	0.009969	-1.42
Nptx2	0.006279	-1.36

$p<0.05$

JNeurosci Accepted Manuscript

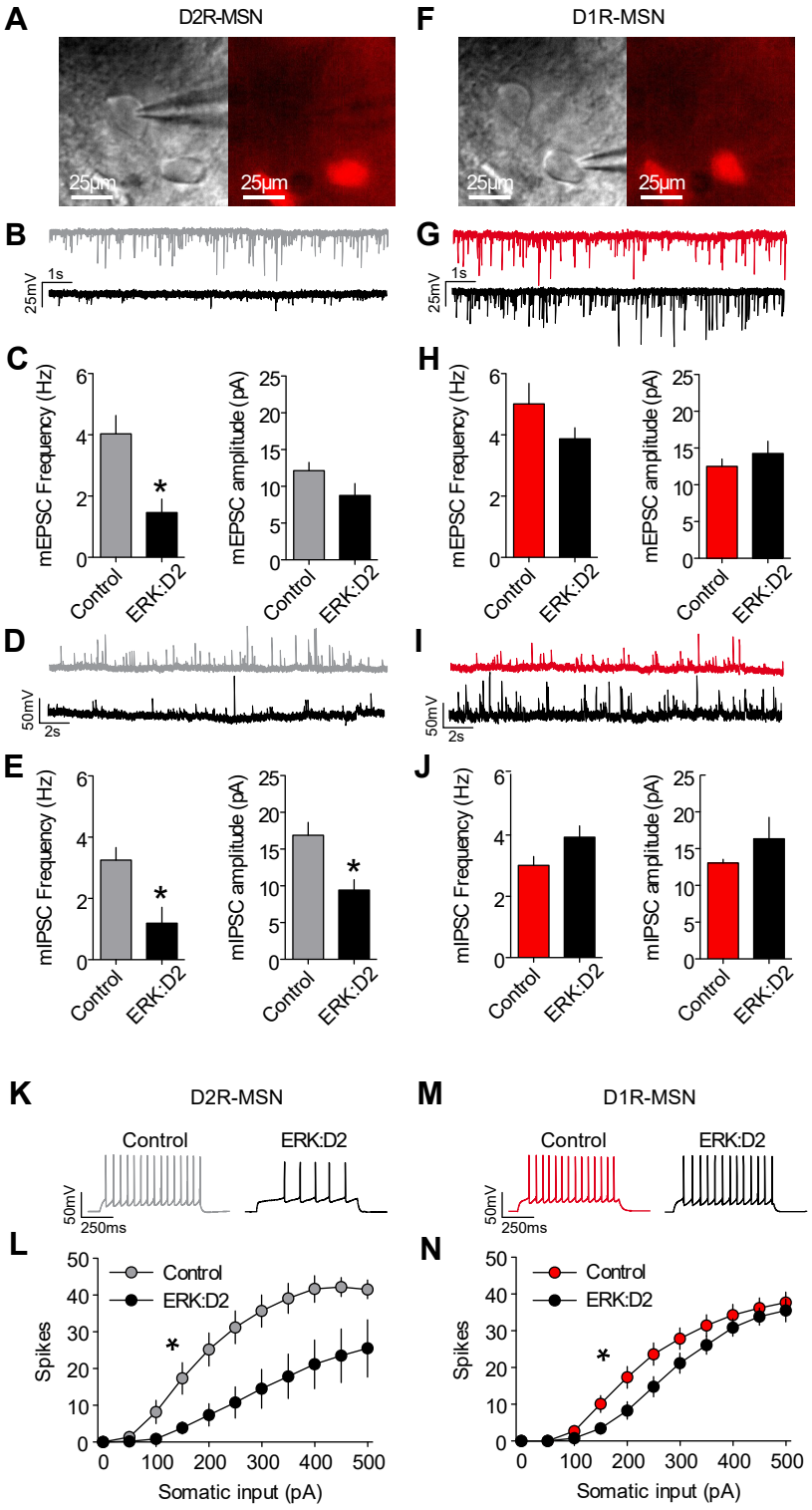

JNeurosci Accepted Manuscript

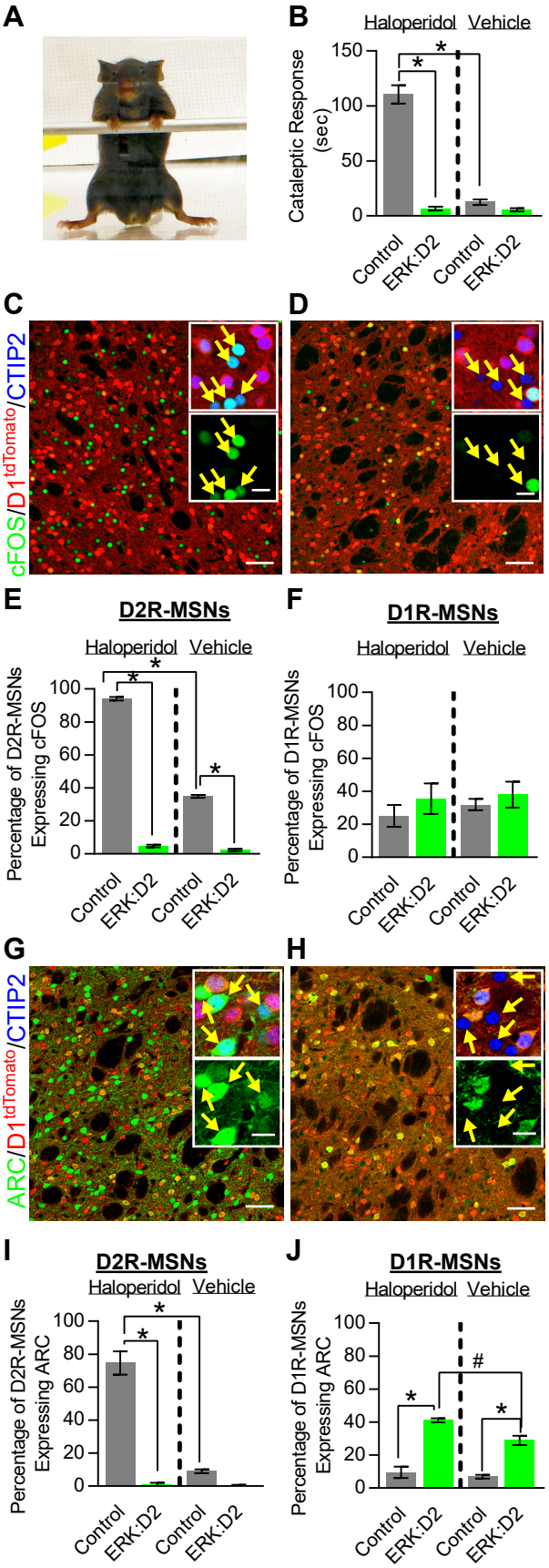

JNeurosci Accepted Manuscript

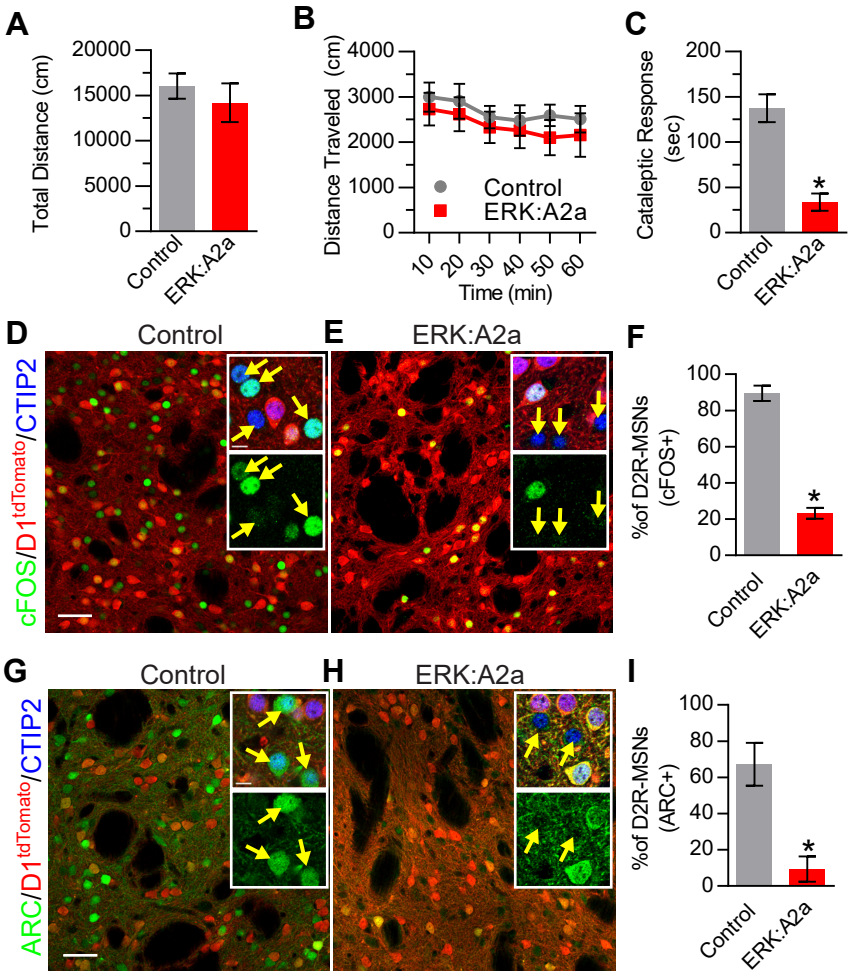

JNeurosci Accepted Manuscript

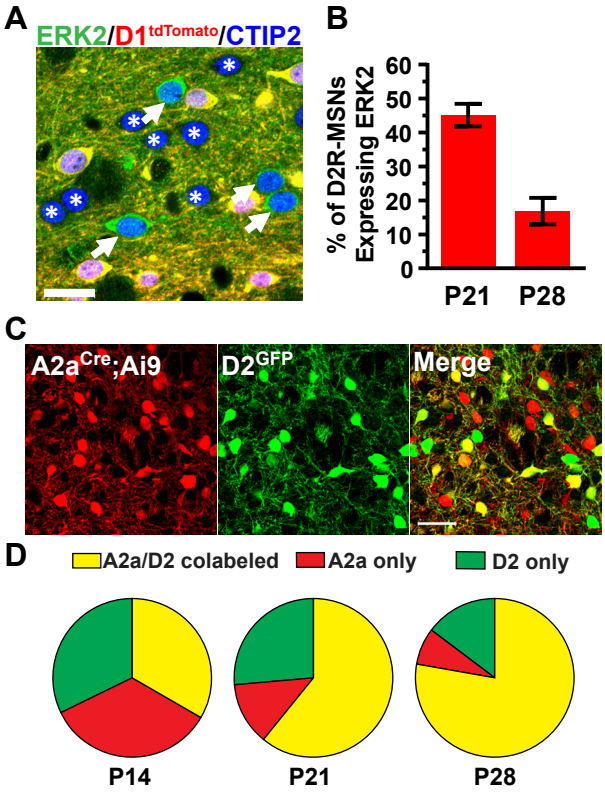

JNeurosci Accepted Manuscript

Table 1

Group	IR(MΩ)	RMP (mV)	Rheo (pA)	Thresh (mV)	Amp (mV)	H.W. (ms)	MaxAPs
D2R Control	126±19	-79.6±2.7	161±20	-38.8±1.3	72.0±3.2	0.87±0.07	45.1±3.3
D2R Erk:D2	115±15	-76.2±4.7	**315±68***	-29.4±4.5	**52.8±7.7***	0.87±0.10	**25.6±7.8***
D1R Control	87±12	-85.6±2.0	204±16	-38.5±2.2	73.1±4.6	0.87±0.06	37.7±2.9
D1R Erk:D2	73±6	-76.9±4.6	252±18	-33.9±2.1	68.3±4.4	0.87±0.05	36.7±2.4